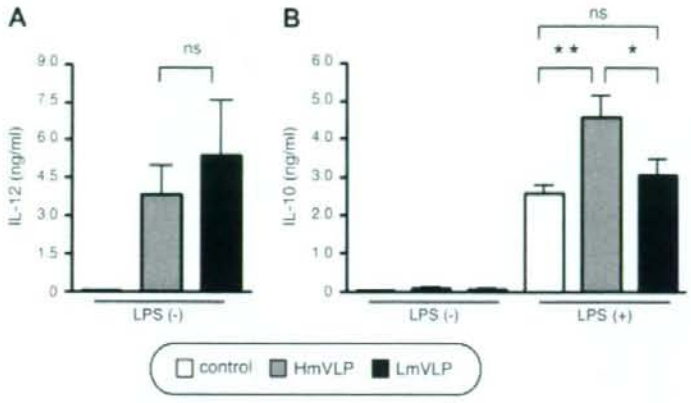

Fig. 4. The effect of yeast VLPs on cytokine production. (A) In the cases of IL-12 responders ($n = 4$), immature MDDCs (2×10^5 cells/200 μl) were incubated with 20 μg/ml HmVLPs (gray bar), LmVLPs (filled bar), or CS (open bar) for 24 h. (B) The MDDCs (2×10^5 cells/200 μl) of IL-12 non-responders ($n = 4$) were incubated with 20 μg/ml HmVLPs (gray bar), LmVLPs (filled bar), or CS (open bar) with or without 100 ng/ml LPS for 24 h. The cytokines produced by these cells were analyzed. Results are presented as the means + SEM. $^*P < 0.05$; $^{**}P < 0.01$; ns, not significant, compared between two groups; one-way ANOVA followed by Bonferroni's t-test ($n = 4$, respectively).

4. Discussion

Antigens expressed by yeast and insect cells contain abundant carbohydrate modifications and are perceived to be excellent vaccine antigens. Consistent with these observations, we previously demonstrated that MDDCs loaded with yeast-derived HIV-1 $p55^{gag}$ VLPs activated Gag-specific $CD8^+$ T cells in chronically-infected HIV patients [14]. Mannosylated antigens taken up by DCs are more efficiently presented to T cells than antigens internalized via fluid phase [15]. However, recent studies have indicated that excessive mannosylation leads to a Th2-dominant response or even suppresses the immune response via a signal from the lectin receptors [17–19]. Therefore, it is important to determine whether the level of mannosylation on VLPs positively or negatively affects the DC-based immune response.

The cell wall of *Saccharomyces cerevisae* is rich in mannoproteins. In this work, we used a yeast mnn9 mutant of the mannosyltransferase, which cannot synthesize completely glycosylated mannoproteins, and demonstrated that VLPs with much reduced mannose induced stronger CTL activation than more heavily mannosylated VLPs derived from wild-type yeast did. Because we used the same amount of Gag protein composed of these VLPs, the difference should be only at the level of glycosylation on VLPs. The efficiency of CTL activation by VLP-pulsed MDDCs was analyzed at 10–20 μg/ml concentration of VLPs. At this concentration, we detected no difference of uptake by FACS analysis. We speculate that the difference, if any, may be not at the level of uptake, but rather during antigen processing or loading to MHC class I. Although we failed to show the difference in the intracellular fate of these VLPs by the current technology, it is still possible that they are differently processed somewhere in the cytoplasm. In this context, it has been demonstrated previously that only a small amount (200 molecules) of peptide and MHC class I complex is enough to be recognized by CTLs [26]. Therefore, even a small difference in the antigen processing process may affect the efficiency of cross-presentation by DCs.

The balance of the Th1/Th2 immune response is influenced by elements such as host conditions and the antigen formulation [27]. LmVLPs induced IL-12 production slightly better than HmVLPs in some donors, whereas in those who do not produce a substantial level of IL-12, LPS-induced IL-10 production was increased by adding HmVLPs, but not by LmVLPs. A number of studies have demonstrated that cytokine production can be altered by the interaction of antigen with lectin receptors and/or toll-like receptors [17–19,28]. For example, Nigou et al. reported that the IL-12 production of DCs induced by LPS was negatively regulated by the engagement of an MR using mannose-capped lipoarabinomannans (the ManLAMs) of *Mycobacteria* [28]. Gringhuis et al. reported that stimulation of DC-SIGN by pathogens such as *Mycobacteria*, fungi, and viruses enhanced toll-like receptor signaling via Raf-1 kinase-dependent acetylation of the transcription factor NF-kB, resulting in strong augmentation of IL-10 mRNA expression by DCs [19]. Thus, stimulation of lectin receptors may preferentially induce IL-10 production in low IL-12 responders. We speculate that a mannosylation-dependent signal affects the Th1/Th2 balance by modulating the cytokine production of DCs, leading to the alternation of CTL activation.

In conclusion, a high level of mannosylation on an antigen may not necessarily be beneficial for CTL induction by DCs. The quantity of carbohydrate chain may alter the Th1/Th2 cytokine balance. DC-based immune therapy that aims to induce CTLs requires optimizing the antigen for the most effective clinical results. Further studies are required to develop the technology for modulating the antigenic property so that it can efficiently induce Th-1 type immune response.

One possible technology may be the modification of the outer structure, amount and variation of sugars moieties on vaccine antigens.

Acknowledgments

We are grateful to T. Sata (Department of Pathology, NIID, Tokyo, Japan) for anti-HIV Gag mAbs (clone 10B5). We are indebted to T. Murakami (AIDS Research Center, NIID, Tokyo, Japan) for excellent technical advice on the subcellular fractionation experiment. This work was supported by a grant from the Ministry of Health, Labour, and Welfare of Japan. F. Mizukoshi receives support from the Japanese Foundation for AIDS Prevention.

References

[1] J. Banchereau, R.M. Steinman, Dendritic cells and the control of immunity, Nature 392 (1998) 245–252.
[2] J. Banchereau, A.K. Palucka, Dendritic cells as therapeutic vaccines against cancer, Nat. Rev. Immunol. 5 (2005) 296–306.
[3] C.G. Figdor, I.J. de Vries, W.J. Lesterhuis, C.J. Melief, Dendritic cell immunotherapy: mapping the way, Nat. Med. 10 (2004) 475–480.
[4] A.G. Thompson, R. Thomas, Induction of immune tolerance by dendritic cells: implications for preventative and therapeutic immunotherapy of autoimmune disease, Immunol. Cell Biol. 80 (2002) 509–519.
[5] T.E. Ichim, R. Zhong, W.P. Min, Prevention of allograft rejection by in vitro generated tolerogenic dendritic cells, Transpl. Immunol. 11 (2003) 295–306.
[6] H. Matsue, M. Kusuhara, K. Matsue, A. Takashima, Dendritic cell-based immunoregulatory strategies, Int. Arch. Allergy Immunol. 127 (2002) 251–258.
[7] J. Colino, C.M. Snapper, Dendritic cells, new tools for vaccination, Microbes Infect 5 (2003) 311–319.
[8] W. Lu, L.C. Arraes, W.T. Ferreira, J.M. Andrieu, Therapeutic dendritic-cell vaccine for chronic HIV-1 infection, Nat. Med. 10 (2004) 1359–1365.
[9] W. Lu, X. Wu, Y. Lu, W. Guo, J.M. Andrieu, Therapeutic dendritic-cell vaccine for simian AIDS, Nat. Med. 9 (2003) 27–32.
[10] R.J. Pomerantz, D.L. Horn, Twenty years of therapy for HIV-1 infection, Nat. Med. 9 (2003) 867–873.
[11] D. Finzi, J. Blankson, J.D. Siliciano, J.B. Margolick, K. Chadwick, T. Pierson, K. Smith, J. Lisziewicz, F. Lori, C. Flexner, T.C. Quinn, R.E. Chaisson, E. Rosenberg, B. Walker, S. Gange, J. Gallant, R.F. Siliciano, Latent infection of CD4+ T cells provides a mechanism for lifelong persistence of HIV-1, even in patients on effective combination therapy, Nat. Med. 5 (1999) 512–517.
[12] B.D. Walker, B.T. Korber, Immune control of HIV: the obstacles of HLA and viral diversity, Nat. Immunol. 2 (2001) 473–475.
[13] A. Duerr, J.N. Wasserheit, L. Corey, HIV vaccines: new frontiers in vaccine development, Clin. Infect. Dis. 43 (2006) 500–511.
[14] Y. Tsunetsugu-Yokota, Y. Morikawa, M. Isogai, A. Kawana-Tachikawa, T. Odawara, T. Nakamura, F. Grassi, B. Autran, A. Iwamoto, Yeast-derived human immunodeficiency virus type 1 p55(gag) virus-like particles activate dendritic cells (DCs) and induce perforin expression in Gag-specific CD8(+) T cells by cross-presentation of DCs, J. Virol. 77 (2003) 10250–10259.
[15] A.J. Engering, M. Cella, D. Fluitsma, M. Brockhaus, E.C. Hoefsmit, A. Lanzavecchia, J. Pieters, The mannose receptor functions as a high capacity and broad specificity antigen receptor in human dendritic cells, Eur. J. Immunol. 27 (1997) 2417–2425.
[16] M.C. Tan, A.M. Mommaas, J.W. Drijfhout, R. Jordens, J.J. Onderwater, D. Verwoerd, A.A. Mulder, A.N. van der Heiden, D. Scheidegger, L.C. Oomen, T.H. Ottenhoff, A. Tulp, J.J. Neefjes, F. Koning, Mannose receptor-mediated uptake of antigens strongly enhances HLA class II-restricted antigen presentation by cultured dendritic cells, Eur. J. Immunol. 27 (1997) 2426–2435.
[17] E. Caparros, P. Munoz, E. Sierra-Filardi, D. Serrano-Gomez, A. Puig-Kroger, J.L. Rodriguez-Fernandez, M. Mellado, J. Sancho, M. Zubiaur, A.L. Corbi, DC-SIGN ligation on dendritic cells results in ERK and PI3K activation and modulates cytokine production, Blood 107 (2006) 3950–3958.
[18] T.B. Geijtenbeek, S.J. Van Vliet, E.A. Koppel, M. Sanchez-Hernandez, C.M. Vandenbroucke-Grauls, B. Appelmelk, Y. Van Kooyk, *Mycobacteria* target DC-SIGN to suppress dendritic cell function, J. Exp. Med. 197 (2003) 7–17.
[19] S.I. Gringhuis, J. den Dunnen, M. Litjens, B. van Het Hof, Y. van Kooyk, T.B. Geijtenbeek, C-type lectin DC-SIGN modulates Toll-like receptor signaling via Raf-1 kinase-dependent acetylation of transcription factor NF-kappaB, Immunity 26 (2007) 605–616.
[20] A. Kawana-Tachikawa, M. Tomizawa, J. Nunoya, T. Shioda, A. Kato, E.E. Nakayama, T. Nakamura, Y. Nagai, A. Iwamoto, An efficient and versatile mammalian viral vector system for major histocompatibility complex class I/peptide complexes, J. Virol. 76 (2002) 11982–11988.
[21] S. Sakuragi, T. Goto, K. Sano, Y. Morikawa, HIV type 1 Gag virus-like particle budding from spheroplasts of Saccharomyces cerevisiae, Proc. Natl. Acad. Sci. USA 99 (2002) 7956–7961.
[22] C.E. Ballou, Isolation, characterization, and properties of *Saccharomyces cerevisiae* mnn mutants with nonconditional protein glycosylation defects, Methods Enzymol 185 (1990) 440–470.
[23] Y. Morikawa, S. Hinata, H. Tomoda, T. Goto, M. Nakai, C. Aizawa, H. Tanaka, S. Omura, Complete inhibition of human immunodeficiency virus Gag myristoylation is necessary for inhibition of particle budding, J. Biol. Chem. 271 (1996) 2868–2873.
[24] Y. Tsunetsugu-Yokota, K. Akagawa, H. Kimoto, K. Suzuki, M. Iwasaki, S. Yasuda, G. Hausser, C. Hultgren, A. Meyerhans, T. Takemori, Monocyte-derived cultured dendritic cells are susceptible to human immunodeficiency virus infection and transmit virus to resting T cells in the process of nominal antigen presentation, J. Virol. 69 (1995) 4544–4547.
[25] C.E. Ballou, Yeast cell wall and cell surface, in: J.N. Stranthern, E.W. Jones, J.R. Broach (Eds.), The Molecular Biology of the Yeast Saccharomyces, Metabolism and Gene Expression, Cold Spring Harbor Laboratory Press, Cold Spring Harbor, NY, 1982, pp. 335–360.
[26] E.R. Christinck, M.A. Luscher, B.H. Barber, D.B. Williams, Peptide binding to class I MHC on living cells and quantitation of complexes required for CTL lysis, Nature 352 (1991) 67–70.
[27] P. Kidd, Th1/Th2 balance: the hypothesis, its limitations, and implications for health and disease, Altern. Med. Rev. 8 (2003) 223–246.
[28] J. Nigou, C. Zelle-Rieser, M. Gilleron, M. Thurnher, G. Puzo, Mannosylated lipoarabinomannans inhibit IL-12 production by human dendritic cells: evidence for a negative signal delivered through the mannose receptor, J. Immunol. 166 (2001) 7477–7485.

Comprehensive Gene Expression Profiling of Peyer's Patch M Cells, Villous M-Like Cells, and Intestinal Epithelial Cells[1]

Kazutaka Terahara,[2*‡] Masato Yoshida,[2*†] Osamu Igarashi,[*‡] Tomonori Nochi,[*‡] Gemilson Soares Pontes,[*] Koji Hase,[§] Hiroshi Ohno,[§] Shiho Kurokawa,[*] Mio Mejima,[*] Naoko Takayama,[*†] Yoshikazu Yuki,[*‡] Anson W. Lowe,[¶] and Hiroshi Kiyono[3*†‡]

Separate populations of M cells have been detected in the follicle-associated epithelium of Peyer's patches (PPs) and the villous epithelium of the small intestine, but the traits shared by or distinguishing the two populations have not been characterized. Our separate study has demonstrated that a potent mucosal modulator cholera toxin (CT) can induce lectin *Ulex europaeus* agglutinin-1 and our newly developed M cell-specific mAb NKM 16-2-4-positive M-like cells in the duodenal villous epithelium. In this study, we determined the gene expression of PP M cells, CT-induced villous M-like cells, and intestinal epithelial cells isolated by a novel approach using FACS. Additional mRNA and protein analyses confirmed the specific expression of glycoprotein 2 and myristoylated alanine-rich C kinase substrate (MARCKS)-like protein by PP M cells but not CT-induced villous M-like cells. Comprehensive gene profiling also suggested that CT-induced villous M-like cells share traits of both PP M cells and intestinal epithelial cells, a finding that is supported by their unique expression of specific chemokines. The genome-wide assessment of gene expression facilitates discovery of M cell-specific molecules and enhances the molecular understanding of M cell immunobiology. *The Journal of Immunology,* **2008, 180: 7840–7846.**

As a unique epithelial cell type specializing in Ag sampling, microfold or membranous cells (M cells) are present in the follicle-associated epithelium (FAE)[4] of both GALT and nasopharynx-associated lymphoid tissue, which act as a major inductive site for Ag-specific mucosal immune responses (1, 2). Recently, we also identified M cells in the small intestinal villous epithelium, at effector sites far from the FAE, suggesting that Ag sampling via villous M cells may be responsible for induction of systemic Ag-specific immune responses, such as IgG production via the oral route (3). Still missing, however, were a characterization of the shared and distinctive traits of Peyer's patches (PPs) and villous M cells and a better understanding of the immunological nature of each.

Recent comprehensive gene expression analyses using microdissected FAE or whole cells dissociated from the FAE identified genes specifically expressed by PP M cells (4–6). Similar data, however, have not been available for villous M cells, in part because sufficient numbers of M cells are difficult to isolate from the surrounding intestinal epithelial cells (IECs). In mice, lectin *Ulex europaeus* agglutinin-1 (UEA-1) possessing affinity for α (1, 2) fucose has been routinely used for the detection of such M cells (3, 7). UEA-1, however, does not alone suffice to identify M cells because it also reacts to goblet cells (3). Our laboratory has recently succeeded in distinguishing M cells from goblet cells by developing a mAb (NKM 16-2-4 mAb) that specifically reacts to murine PP and villous M cells but not goblet cells and IECs (8). Furthermore, our recent separate studies have demonstrated that oral administration of cholera toxin (CT) as mucosal adjuvant resulted in the induction of NKM 16-2-4 mAb$^+$ and UEA-1$^+$ M-like cells, which have pocket structure and Ag uptake ability, in the duodenal villous epithelium (Terahara et al., submitted for publication). These recent advances in our understanding of M cells allowed us to define gene expression profiles capable of distinguishing PP M cells, CT-induced villous M-like cells, and IECs.

Materials and Methods

Animals

BALB/c mice were purchased from Japan SLC. These mice were maintained under specific pathogen-free conditions in horizontal flow cabinets in our experimental animal facility at the University of Tokyo. Following a previously established protocol (9, 10), CT (List Biologic Laboratories) was dissolved in PBS (20 μg/mouse) and then orally administered to BALB/c mice. Two days after CT administration, mice were used for experiments. All animal experiments were approved by the Animal Care and Use Committee of University of Tokyo.

Lectins and Abs for the detection of M cells

The following fluorescence-conjugated lectins and Abs were used for the identification of PP and villous M cells by FACS and histochemistry: PE-conjugated UEA-1 (Biogenesis), rhodamine-conjugated UEA-1 (Vector

[*]Division of Mucosal Immunology, Department of Microbiology and Immunology, The Institute of Medical Science and [†]Department of Medical Genome Science, Graduate School of Frontier Science, The University of Tokyo, Tokyo; [‡]Core Research for Evolutional Science and Technology, Japan Science and Technology Corporation, Saitama; and [§]Laboratory of Epithelial Immunobiology, Research Center for Allergy and Immunology, Institute of Physical and Chemical Research, Yokohama, Japan; and [¶]Department of Medicine, Stanford University, Stanford, CA 94305

Received for publication February 12, 2007. Accepted for publication April 3, 2008.

The costs of publication of this article were defrayed in part by the payment of page charges. This article must therefore be hereby marked *advertisement* in accordance with 18 U.S.C. Section 1734 solely to indicate this fact.

[1] This work was supported in part by grants from Core Research for Evolutional Science and Technology of the Japan Science and Technology Corporation, the Ministry of Education, Science, Sports, and Culture, and the Ministry of Health and Welfare in Japan.

[2] K.T. and M.Y. contributed equally to this work and share first authorship.

[3] Address correspondence and reprint requests to Dr. Hiroshi Kiyono, Division of Mucosal Immunology, Department of Microbiology and Immunology, The Institute of Medical Science, The University of Tokyo, 4-6-1 Shirokanedai, Minato-ku, Tokyo 108-8639, Japan. E-mail address: kiyono@ims.u-tokyo.ac.jp

[4] Abbreviations used in this paper: FAE, follicle-associated epithelium; 7-AAD, 7-amino actinomycin; CKLF, chemokine-like factor; CT, cholera toxin; DAPI, 4′-6-diamidino-2-phenylindole; IEC, intestinal epithelial cell; IEL, intraepithelial lymphocyte; ISH, in situ hybridization; MLP, myristoylated alanine-rich C kinase substrate (MARCKS)-like protein; PP, Peyer's patch; UEA-1, *Ulex europaeus* agglutinin-1; WGA, wheat germ agglutinin.

Laboratories), biotin-conjugated UEA-1 (Vector Laboratories), FITC-conjugated wheat germ agglutinin (WGA) (Vector Laboratories), FITC-conjugated or biotin-conjugated M cell-specific NKM 16-2-4 mAb (8), and allophycocyanin-Cy7-conjugated anti-mouse CD45 mAb (30-F11; BD Biosciences).

Isolation of PP M cells, CT-induced villous M-like cells, and IECs

PPs from the naive duodenum and PP-free segments from the duodenum of naive or CT-administered mice were washed with cold PBS. Cells were dissociated from the small intestinal epithelium using a previously described mechanical procedure with some modifications (11). In brief, the tissues were incubated in PBS containing 0.5 mM EDTA with a stirrer for 10 min at 37°C. More than 90% of the dissociated cells survived as confirmed by a trypan blue exclusion test. The cells were stained with 1 μg/ml FITC-conjugated NKM 16-2-4 mAb, 5 μg/ml PE-conjugated UEA-1, and 1 μg/ml allophycocyanin-Cy7-conjugated anti-mouse CD45 mAb for 40 min before being reacted with 7-amino actinomycin (7-AAD; BD Biosciences) diluted 1/5 in DMEM containing 10% FCS for 10 min on ice. After washing with DMEM containing 10% FCS, the stained cells were analyzed using a flow cytometer FACSAria (BD Biosciences), and suitable cell populations gated on $CD45^+$ and $7\text{-}AAD^-$ cells were sorted.

DNA microarray analysis

Total RNA was extracted from the freshly isolated PP M cells, CT-induced villous M-like cells, and IECs of BALB/c mice using a High Pure RNA Tissue kit (Roche). Biotinylated cRNA was prepared using a two-cycle target-labeling assay in accordance with the protocol of the manufacturer (Affymetrix). The cRNA was hybridized with DNA probes on a GeneChip Mouse Genome 430 2.0 array (Affymetrix), washed, and fluorescence-labeled in accordance with the standard amplification protocol for eukaryotic targets developed by Affymetrix. The arrays were scanned with a GeneChip Scanner 3000 7G (Affymetrix). The fluorescence intensity of each probe was taken to represent the raw expression level and was quantified using GeneChip Operating software (Affymetrix). Data obtained from three independent experiments for PP M cells, CT-induced villous M-like cells, and IECs were normalized and statistically analyzed by Welch's ANOVA using GeneSpring 7.3.1 software (Silicon Genetics). In addition, both qualitative indices ("Present Call," "Marginal Call," and "Absent Call") based on *p*-value and a quantitative index (raw value) were also determined using GeneSpring 7.3.1 software. All microarray data described in this study have been deposited in the National Center for Biotechnology Information Gene Expression Omnibus database (www.ncbi.nlm.nih.gov/geo/) with the accession no. GSE7838.

In situ hybridization (ISH)

DNA fragments encoding GP2 (GenBank: NM_025989) and myristoylated alanine-rich C kinase substrate (MARCKS)-like protein (MLP; GenBank: NM_010807) were amplified by PCR from PP FAE-derived cDNA. The following sets of primers were used: *GP2*, sense, 5′-GGGTGATGGAGG AGTGAAGA-3′, anti-sense, 5′-CTCCAGGATGTTCCCACAGT-3′; and *MLP*, sense, 5′-*AATTAACCCTCACTAAAGGG*GAAGGCCAACGGACAG GAGA-3′, anti-sense, 5′-*TAATACGACTCACTATAGGG*CTTCTTGGGG GTCTCCTTGG-3′ (T3 and T7 promoter sequences are shown by italics). The PCR products for GP2 were subcloned into a pCR4-TOPO vector (Invitrogen). After sequencing, digoxigenin-labeled sense and anti-sense RNA probes were transcribed in vitro from the subcloned plasmids or from T3 and T7 promoter-conjugated PCR products with DIG RNA labeling mix (Roche). Paraffin-embedded sections of small intestinal tissues (6 μm) from naive BALB/c mice were obtained from Genostaff. ISH was performed as previously described (12). The bound probes were detected with BM purple AP substrate (Roche), before being counterstained with Kernechtrot stain solution (Muto Pure Chemicals) or reacted with 0.25 μg/ml biotin-conjugated UEA-1 at 4°C overnight after treatment with 3% H_2O_2. The sections labeled with biotin-conjugated UEA-1 were further reacted with HRP-conjugated streptavidin, followed by staining with 3,3′ diaminobenzidine (Vector Laboratories).

Generation of GP2- and MLP-specific Abs

For the generation of GP2- and MLP-specific Abs, the open reading frames of *GP2* and *MLP* genes were amplified by PCR from PP FAE-derived cDNA. The following sets of primers were used: *GP2*, sense, 5′-GACA TG*CTAGC*ATGAAAAGGATGGTGGGTTGTGAC-3′, anti-sense, 5′-GT ATC*GAATTC*TCAGAACAGTAGAGCCAGGAAGAC-3′; and *MLP*, sense, 5′-TGACTG*AATTC*ATGGGCAGCCAGAGCTCTAAGGCT-3′, anti-sense, 5′-TACAT*GTCGAC*CTACTCATTCTGCTCAGCACTGGC-3′.

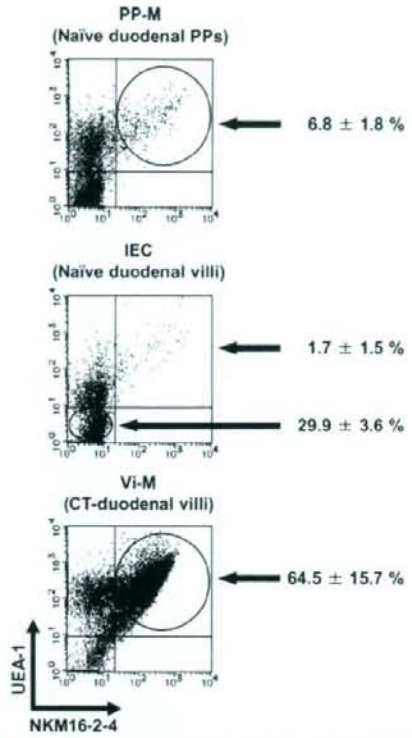

FIGURE 1. Frequency of PP M cells (PP-M) and CT-induced villous M-like cells (Vi-M) in the duodenal epithelium. Dot plots are shown by NKM 16-2-4-FITC and UEA-1-PE staining gated on $CD45^+$ and $7\text{-}AAD^-$ duodenal epithelial cell populations from naive BALB/c mice or from those that had been orally treated with CT. PP-M ($NKM\ 16\text{-}2\text{-}4^+$ and $UEA\text{-}1^+$), Vi-M ($NKM\ 16\text{-}2\text{-}4^+$ and $UEA\text{-}1^+$), and IEC ($NKM\ 16\text{-}2\text{-}4^-$ and $UEA\text{-}1^-$) were isolated by FACS. Numbers are the mean percentage ± SD in $CD45^+$ and $7\text{-}AAD^-$ epithelial cell populations from three independent experiments.

[*Nhe*I and *Eco*RI (*GP2*), and *Eco*RI and *Sal*I (*MLP*) restriction enzyme sites are shown by italics]. For generation of GP2-specific mAbs, amplified *GP2* gene was subcloned into pIRES2-EGFP vector (BD Biosciences) and the plasmid (pIRES2-GP2-EGFP) was then introduced in rat IEC line IEC-6 (ATCC, CRL-1592). After 2 days of transformation, EGFP-positive cells were purified by FACSAria and injected into the footpads of SD rats (1×10^6 cells/rat) five times at 2-wk intervals with TiterMax Gold (TiterMax) as an adjuvant. Four days after the final immunization, lymphocytes isolated from inguinal lymph node of the immunized rats were fused with P3×63-AG8.653 myeloma cells (ATCC, CRL-1580) in the presence of 50% (w/v) polyethylene glycol 1500 (Roche). Established hybridomas were injected into Crlj; CD1-*Foxn1*^{nu} mice and mAbs were purified from ascites by using Protein G-Sepharose (GE Healthcare). For generation of MLP-specific polyclonal Abs, the amplified *MLP* gene was subcloned into pGEX-4T-1 (GE Healthcare) and the plasmid (pMLP-GEX-4T-1) was then introduced in *Escherichia coli* DH5α. After induction of MLP expression with 0.1 mM isopropyl β-D-thiogalactoside, the GST-fused MLP was purified on a Glutathione-Sepharose 4B (GE Healthcare) and subsequently removed the GST-tag with thrombin (GE Healthcare). The purified rMLP was then immunized into New Zealand white rabbits and anti-MLP pAbs were purified from the antiserum by using rMLP-conjugated TOYOPEARL AF-Tresyl-650M (Tosoh).

Histochemical analysis

The histochemical analyses were performed with whole-mount tissues and frozen-section specimens prepared from mucus-free tissues fixed with 4% paraformaldehyde in PBS as previously described (3). For GP2 staining,

A

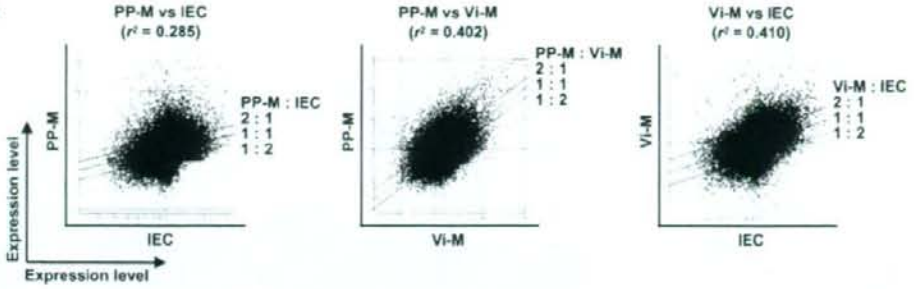

B

Group	Description	Criterion
A	PP-M-significant	1. "Present" or "Marginal Call" together with ≥ 100 raw value is shown in a cell fraction but not in the other two cell fractions.
B	Vi-M-significant	2. A normalized expression signal in a cell fraction is two-fold or higher than that seen in the other two cell fractions.
C	IEC-significant	
D	Sharing between PP-M and Vi-M	1. "Present" or "Marginal Call" together with ≥ 100 raw value is shown in two cell fractions but not in another cell fraction.
E	Sharing between PP-M and IEC	2. Each normalized expression signal in two cell fractions is two-fold or higher than that in another cell fraction.
F	Sharing between Vi-M and IEC	
G	Sharing in all cell fractions	1. "Present" or "Marginal Call" together with ≥ 100 raw value is shown in all cell fractions.

C

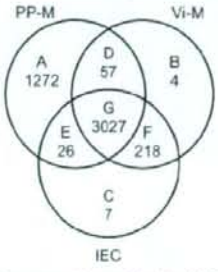

FIGURE 2. Gene expression profiles for PP M cells (PP-M), CT-induced villous M-like cells (Vi-M), and IECs. *A*, Scatter plots of the normalized expression level on each DNA microarray probe for PP-M and IEC, PP-M and Vi-M, and Vi-M and IEC with correlation coefficients (r^2). *B*, Grouping of probes based on their significance for PP-M, Vi-M, and IEC using the criteria outlined in the qualitative ("Present Call" or "Marginal Call") and quantitative (raw value) indices as assessed by GeneSpring 7.3.1 software. *C*, Venn diagram showing the categorization of significant probes into seven groups (Group A–G).

the specimens were incubated with 1 μg/ml rat anti-GP2 mAb (10F5-9-2) or the isotype control Ab (rat IgG2a; BD Biosciences) at 4°C overnight. For MLP staining, tissue sections were incubated with 10 μg/ml anti-MLP pAb or normal rabbit IgG at 4°C overnight. The specimens were then treated with 3 μg/ml Cy5-conjugated donkey anti-rat IgG or 3 μg/ml Cy5-conjugated donkey anti-rabbit IgG (Jackson ImmunoResearch Laboratories) together with 10 μg/ml tetramethylrhodamine isothiocyanate-conjugated UEA-1 (Vector Laboratories) and/or 5 μg/ml FITC-conjugated WGA (Vector Laboratories) for 1 h at room temperature. Finally, the section specimens were reacted with 400 ng/ml 4′-6-diamidino-2-phenylindole (DAPI; Sigma-Aldrich) and the signal was observed under a confocal laser-scanning microscope (TCS SP2; Leica). For counterstaining with our recently established M cell-specific mAb (NKM 16-2-4; rat IgG2c), the same section specimens were incubated with 5 μg/ml biotin-conjugated NKM 16-2-4 at 4°C overnight followed by 1.25 μg/ml HRP-conjugated streptavidin (Pierce) for 1 h at room temperature. The signal was then developed with 3,3′ diaminobenzidine and the nucleus was finally stained with hematoxylin.

Results

Isolation of PP M cells, CT-induced villous M-like cells, and IECs by FACS

FACS analysis demonstrated that the large forward-scatter CD45$^-$ cell population could be divided into three subpopulations by NKM 16-2-4 mAb and UEA-1 staining (Fig. 1). Because of the known specificities of NKM 16-2-4 mAb and UEA-1, cells positive for NKM 16-2-4 and UEA-1 were identified as M cells (or M-like cells) in this study. In the CD45$^-$ epithelial cell population isolated from the duodenum of naive BALB/c mice, the frequency of PP M cells averaged 7%. Perhaps due to the nature of the isolation technique used, the harvest of PP M cells far outstripped that of villous M cells, the frequency of the latter being so low (1.7 ± 1.5%) as to render harvest extremely difficult. We recently found that the number of villous M-like cells could be increased by oral administration of CT (64.5 ± 15.7% and Terahara et al., submitted for publication), and so decided to use the villous M-like cells induced by CT treatment for this DNA microarray analysis. A FACS with a purity of 90–99% was used to isolate PP M cells (NKM 16-2-4$^+$/UEA-1$^+$), CT-induced villous M-like cells (NKM 16-2-4$^+$/UEA-1$^+$), and IECs (NKM 16-2-4$^-$/UEA-1$^-$).

Assessment of gene expression profiling of PP M cells, CT-induced villous M-like cells, and IECs

DNA microarrays containing 45,101 probes were used to determine the comprehensive gene expression of PP M cells, CT-induced villous M-like cells, and IECs. Comparison of these

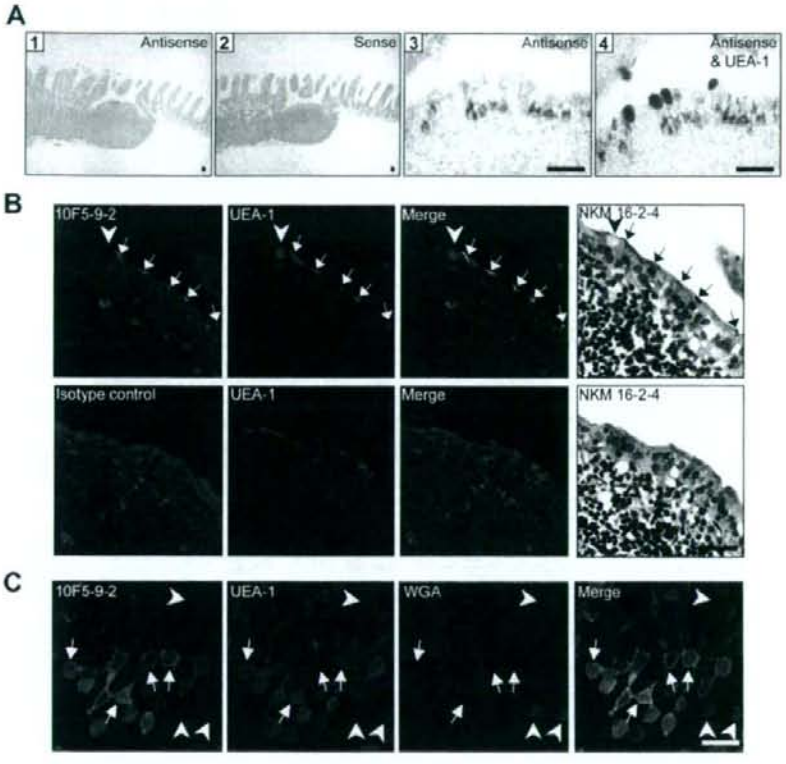

FIGURE 3. GP2 was specifically expressed by PP M cells in the small intestine. *A*, ISH for GP2 mRNA with positive signals (blue) of hybridized anti-sense or sense cRNA probes on duodenal PPs and adjacent villi of naive BALB/c mice. Tissues were also counterstained with Kernechtrot (pink, *1* and *2*) or labeled with UEA-1-HRP before being stained with 3,3′ diaminobenzidine (brown, *4*). *3* and *4*, High magnification of a PP FAE before (*3*) and after (*4*) labeling with UEA-1. Scale bar = 200 μm (*1* and *2*) and 40 μm (*3* and *4*). *B*, Confocal images of frozen sections of PPs stained with anti-GP2-specific mAb (10F5-9-2) or isotype control (rat IgG2a). The specific expression of GP2 in M cells was confirmed by counterstaining with our recently established M cell-specific mAb (NKM 16-2-4). Arrows and arrowheads show M cells and goblet cells, respectively. Scale bar = 30 μm. *C*, Confocal images of whole-mount duodenal PP domes stained with anti-GP2-specific mAb (10F5-9-2), UEA-1, and WGA. Scale bar = 30 μm.

profiles revealed correlation coefficients of 0.285 for PP M cells and IECs, of 0.402 for PP M cells and CT-induced villous M-like cells, and of 0.410 for CT-induced villous M-like cells and IECs (Fig. 2*A*). Based on the constructed gene profiling, we categorized probes showing significant expression into seven groups (Groups A-G) using our own criteria (Fig. 2*B*). The 1272, 4, and 7 probes were regarded as significant for PP M cells (Group A), CT-induced villous M-like cells (Group B), and IECs (Group C), respectively (Fig. 2*C*). The relative expression levels and gene names of the significant probes are provided in Supplementary Table I.[5] Our gene-profiling database allowed us to confirm previous findings that Group A includes the transcripts of peptidoglycan recognition protein-S, secretory granule neuroendocrine protein 1, and annexin V that are specifically expressed by PP M cells (4–6).

Specific expression of GP2 by PP M cells

In an effort to identify molecules that could be expressed on the apical surface of PP M cells, we looked for genes showing a higher expression level in Group A. During the ISH analysis, we found that GP2 mRNA was specifically expressed in the FAE of PPs throughout the small intestine (Fig. 3*A*, *1*) and that its expression was distinctively colocalized with UEA-1$^+$ M cells (Fig. 3*A*, *3* and *4*). A negative control using sense cRNA probes did not show any positive signals (Fig. 3*A*, *2*). Immunohistochemical analysis with newly established anti-GP2-specific mAb (10F5-9-2) revealed that the GP2 protein was highly expressed in UEA-1$^+$ PP M cells (Fig. 3*B*). A negative control using isotype rat IgG2a did not show any positive signals in the dome epithelium of PPs (Fig. 3*B*). The expression of GP2 in M cells was further confirmed by counterstaining with our recently established M cell-specific mAb NKM 16-2-4 (Fig. 3*B*). Supporting the histochemical analyses, whole-mount staining analysis also demonstrated GP2 was expressed on the apical surface of UEA-1$^+$ PP M cells, which were not recognized by enterocyte-reactive lectin WGA (Fig. 3*C*). Supporting the gene profiling data (Supplementary Table I), GP2 protein was not detected in CT-induced villous M-like cells (data not shown).

Unique expression of MLP by PP M cells in the small intestine

Candidates for FAE-specific genes including *MLP* (also known as *MacMARCKS* or *MRP*) have been previously proposed (5, 6). Most of these genes together with *MLP* could be identified as PP M cell-significant genes by the DNA microarray analysis (Supplementary Table I). The subsequent ISH analysis demonstrated a unique expression pattern of MLP mRNA in the small intestine, i.e., MLP mRNA was detected in the FAE and B cell zones of PPs throughout the small intestine (Fig. 4*A*, 1). A negative control using sense cRNA probes did not show any positive signals (Fig. 4*A*, 2). In the FAE, the expression of MLP mRNA was exclusively colocalized with UEA-1$^+$ M cells (Fig. 4*A*, 3 and 4). Immunohistochemical analysis further elucidated the complicated expression pattern of MLP, revealing that the MLP protein was also found in B cell zones and the cytoplasm of M cells in PPs throughout the small intestine (Fig. 4*B*), but not in CT-induced villous M-like cells (data not shown). A negative control using normal rabbit IgG did not show any positive signals (Fig. 4*B*).

[5] The online version of this article contains supplemental material.

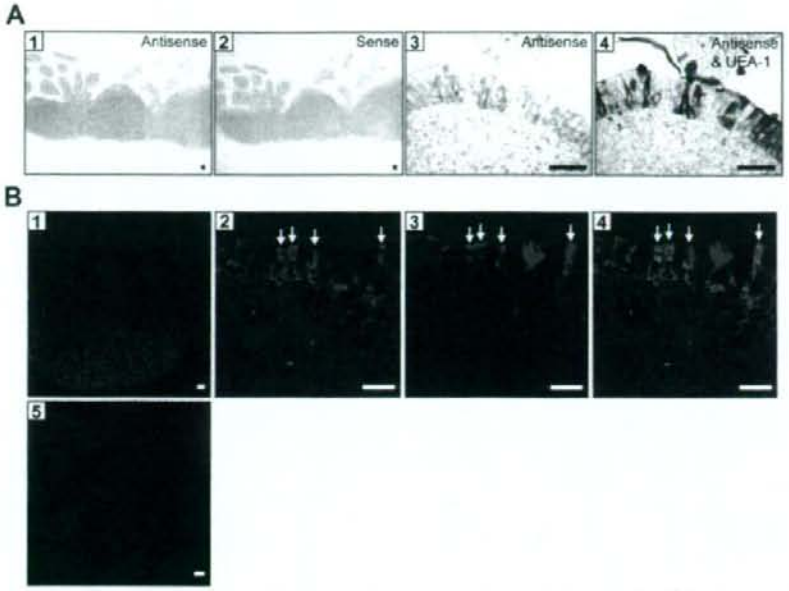

FIGURE 4. MLP was expressed by M cells and by the B cell zones of PPs but not by villi. *A*, ISH for MLP mRNA with positive signals (blue) of hybridized anti-sense or sense cRNA probes on duodenal PPs and adjacent villi of naive BALB/c mice. Tissues were also counterstained with Kernechtrot (pink, *1* and *2*) or labeled with UEA-1-HRP before being stained with 3,3′ diaminobenzidine (brown, *4*). *3* and *4*, High magnification of a PP FAE before (*3*) and after (*4*) labeling with UEA-1. Scale bar = 200 μm (*1* and *2*) and 40 μm (*3* and *4*). *B*, Confocal images of frozen sections of duodenal PPs stained with anti-MLP-specific pAb or control rabbit IgG. Confocal images of frozen sections of duodenal PPs from naive BALB/c mice labeled with UEA-1-rhodamine, DAPI, and immune complexes of FITC-labeled anti-rabbit IgG secondary Ab with anti-MLP polyclonal Ab or normal rabbit IgG. *1* and *5*, Merged images of DAPI (blue) and MLP (green) (*1*) or normal rabbit IgG (green) (*5*). *2–4*, High magnification of a PP FAE. *2*, Merged image of DAPI-(blue) and MLP (green)-staining. *3*, Single image of UEA-1-staining (red). *4*, Merged image of (*2*) and (*3*). Arrows show PP M cells expressing MLP. Scale bar = 100 μm (*1*), 50 μm (*5*), and 10 μm (*2–4*).

Unique expression of chemokines in PP M cells and/or CT-induced villous M-like cells

Focusing on chemokines whose presence was statistically identified regardless of the raw value, we found seven chemokines to be expressed by PP M cells and/or CT-induced villous M-like cells (Table I). In addition to the previously reported CCL9 and CCL20 that are expressed by the M cell-containing PP FAE (13–15), we found significant expression of CXCL13 and chemokine-like factor (CKLF) in PP M cells. Although CT-induced villous M-like cells and IECs constitutively expressed CCL6 and CCL28, the expression level of these chemokines was highest in PP M cells (thereby categorized in Group G; Fig. 2, *B* and *C*). Next, we also examined the expression pattern of chemokines in CT-induced villous M-like cells, finding, as in PP M cells, an up-regulation of CCL9, CKLF, and CCL6 mRNAs. Their raw values and expression levels were higher than those seen in IECs (Table I). Furthermore, CT-induced villous M-like cells showed the highest expression of CXCL16 mRNA, with expression levels 1.9–2.5-fold higher than in PP M cells and 2.1–2.3-fold higher than in IECs (Table I).

Table I. *Chemokines expressed by PP M cells and/or CT-induced villous M-like cells*[a]

Name	GenBank	Affymetrix Probe No.	Group (see Fig. 2C)	Relative Expression Level against IEC	
				PP-M	Vi-M
CCL9	AF128196	1417936_at	A	124.8	7.0
CXCL13	AF030636	1417851_at	A	64.4	-
CKLF	BE852312	1436242_a_at	A	52.2	8.3
CCL6	AV084904	1420249_s_at	G	30.4	5.1
	BC002073	1417266_at	G	12.5	4.6
CCL20	AF099052	1422029_at	A	10.9	-
CCL28	BE196980	1455577_at	G	2.8	0.7
CXCL16	BC019961	1449195_s_at	G	1.1	2.1
		1418718_at	G	0.9	2.3

[a] Expression levels on probes identified as "Present Call" in PP M cells (PP-M) or CT-induced villous M-like cells (Vi-M) were compared with those in IECs. Minus indicated no expression in Vi-M and IECs. CKLF, Chemokine-like factor.

Discussion

In this study, we combined the advanced techniques of M cell purification and DNA microarrays to construct a gene-profiling database for PP M cells, CT-induced villous M-like cells, and IECs. The lack of M cell-specific markers has long presented an obstacle to the isolation of M cells. We overcame this barrier by using M cell-specific NKM 16-2-4 mAb. Our knowledge that villous M (or M-like) cells, usually low frequency in the duodenum, could be increased by CT allowed us to separately isolate PP M cells, CT-induced villous M-like cells, and IECs using FACS. Of course, we cannot yet exclude the possibility that individual cell-sorted fractions were mildly contaminated by other cell types; however, we regard the database as reliable because most of the previously reported PP M cell-specific genes encoding peptidoglycan recognition protein-S, secretory granule neuroendocrine protein 1, and annexin V (4–6) were found in the PP M cell-significant group (Group A). Thus, the gene-profiling database presented

here has several advantages: it appears reliable because it was capable of confirming already established findings; it includes villous M (or M-like) cells as well as PP M cells and IECs; and it is based on a purified cell population. These advantages could make this gene-profiling database a reliable and useful tool for identifying new molecules expressed by M cells and for deepening our understanding of M cell immunobiology.

A mucosal vaccine delivery system targeting PP M cells would be more effective at generating not only efficient mucosal but also systemic immunity. When UEA-1 was used as an Ag delivery vehicle, the administration of PP M cell-targeted Ags induced Ag-specific mucosal and systemic immune responses (16) despite the cospecificity of the lectin for M cells and goblet cells (3). The gene-profiling database was, therefore, used to look for candidate target molecules in the vaccine delivery system. We focused on GP2, which is a GPI-anchored protein expressed at a higher level in Group A. GP2 is associated with lipid rafts, is sorted to the apical plasma membrane (17), and is likely to possess a similar distribution in PP M cells. Additional mRNA and protein analyses by ISH and immunohistochemistry identified the specific expression of GP2 in the apical plasma membrane of PP M cells. Although the role played by GP2 in a unique Ag-sampling system of PP M cells remains obscure, GP2 is not required for PP M cell development, as evidenced by the presence of M cells in the FAE of PPs from $GP2^{-/-}$ mice (data not shown). Taken together, these findings support the candidacy of GP2 as an M cell-targeting molecule. If it is in fact confirmed to be so, it could greatly contribute to the development of a mucosal vaccine delivery system.

In addition to the identification of GP2, reliance of the gene-profiling database is further supported by the identification of specific expression of MLP by PP M cells. Not only *MLP* but also other genes have been previously reported as FAE-specific genes (5, 6). Using DNA microarray analysis, we were able to identify most such genes, including *MLP*, as PP M cell-significant genes. This study demonstrated for the first time the histological distribution of expressed MLP mRNA and protein in the small intestine. MLP, a member of protein kinase C substrates, binds calcium/calmodulin and actin (18, 19), and has been implicated in integrin-dependent phagocytosis by macrophages (20, 21). However, that contention was challenged in another study by Underhill and coworkers (22) using $MLP^{-/-}$ macrophages. Interestingly, $\beta 1$ integrin, which is expressed by the apical membrane of PP M cells but not of IECs in the murine small intestine, is involved in the uptake of *Yersinia* by PP M cells via integrin-invasin binding (23). Thus, MLP may also account for the Ag uptake/sampling process, including integrin-dependent Ag uptake, of M cells located within the FAE of PPs.

Our constructed gene profiling also provides additional information for M cell immunobiology. Both PP and villous M cells contain in their basolateral region immunocompetent cells characterized by a pocket formation (3, 24), the contents of which are influenced by the repertoire of chemokines expressed by M cells. So far, three chemokines, CCL9, CCL20, and CXCL16, have been reported to be specifically expressed by the M cell-containing FAE of PPs and to contribute to the spatial distribution of dendritic cells or T cells in the subepithelial dome as well as in the basolateral pocket regions of M cells (13–15, 25). Our examination for the gene expression pattern of chemokines using the gene-profiling database showed that CXCL13, CKLF, CCL6, and CCL28, in addition to CCL9 and CCL20, are specifically or highly expressed by PP M cells, suggesting that CXCL13, CKLF, CCL6, and CCL28 may also play a role in regulating the recruitment of various immunocompetent cells into the pocket region of PP M cells.

Noticeably, CT-induced villous M-like cells share with PP M cells the expression of certain chemokines, including CCL6, CCL9, and CKLF. Furthermore, the highest expression of CXCL16 mRNA was observed in CT-induced villous M-like cells, although CXCL16 has previously been shown to be specifically expressed in the FAE of PPs (25). This discrepancy may result from our exclusive use of duodenal tissues for the analysis of M cell gene profiling. CXCL16 is a chemoattractant for activated $CD8^+$ T cells and, to a lesser extent, for activated $CD4^+$ T cells (25, 26); the CXCL16 receptor is expressed by intraepithelial lymphocytes (IELs) (26). In the small intestine, the distribution patterns for $CD4^+$ and $CD8^+$ T cells are distinct, with $CD4^+$ T cells primarily located in the lamina propria and $CD8^+$ T cells residing along the epithelium (27). When CT was orally administered, $CD8^+$ IELs were rapidly and transiently depleted (28). Interestingly, we observed that $CD8^+$ IEL numbers recovered following the generation of CT-induced villous M-like cells (data not shown). Therefore, our current finding that CT-induced villous M-like cells express a higher level of CXCL16 makes it plausible that $CD8^+$ T cells are retained in the intestinal epithelium, mainly into the pocket of villous M-like cells. Furthermore, up-regulation of CCL9, CKLF, CCL6, and CXCL16 in CT-induced villous M-like cells could account for the CT-induced recruitment of immunocompetent cells to the site of Ag sampling from the intestinal lumen via CT-induced villous M-like cells.

Although the development mechanism of villous M cells remains unclear, we hypothesize that villous M cells are differentiated from IECs by exogenous stimuli because oral CT administration resulted in the induction of villous M-like cells in the middle to upper regions of villi (Terahara et al., submitted for publication), i.e., where IECs normally migrate from the crypts to the villus (29). Our hypothesis is also informed by the suggestions offered by other groups that IECs in the FAE of PPs could be converted to M cells by bacterial infection and inflammation (30, 31). We propose that CT-induced villous M-like cells have a gene expression pattern that is intermediate between PP M cells and IECs, as evidenced by the very similar correlation coefficient values obtained when the comprehensive gene profile of CT-induced villous M-like cells was compared with that of PP M cells (r^2 = 0.402) and IECs (r^2 = 0.410). The intermediate nature of CT-induced villous M-like cells between PP M cells and IECs is further confirmed by chemokine expression profiles. In this study, we have attempted to use gene profiling to elucidate the development mechanism of villous M cells.

In conclusion, our gene-profiling database should prove a valuable tool in identifying suitable M cell-targeting molecules, thereby speeding the development of a mucosal vaccine delivery system as well as allowing for a better understanding of M cell immunobiology.

Acknowledgments

We thank the members of our laboratory for technical advice and helpful discussions. We also extend our thanks to Dr. K. McGhee for editorial help.

Disclosures

The authors have no financial conflict of interest.

References

1. Gebert, A., H. J. Rothkötter, and R. Pabst. 1996. M cells in Peyer's patches of the intestine. *Int. Rev. Cytol.* 167: 91–159.
2. Neutra, M. R., A. Frey, and J. P. Kraehenbuhl. 1996. Epithelial M cells: gateways for mucosal infection and immunization. *Cell* 86: 345–348.
3. Jang, M. H., M. N. Kweon, K. Iwatani, M. Yamamoto, K. Terahara, C. Sasakawa, T. Suzuki, T. Nochi, Y. Yokota, P. D. Rennert, et al. 2004. Intestinal villous M

cells: an antigen entry site in the mucosal epithelium. *Proc. Natl. Acad. Sci. USA* 101: 6110–6115.
4. Lo, D., W. Tynan, J. Dickerson, J. Mendy, H. W. Chang, M. Scharf, D. Byrne, D. Brayden, L. Higgins, C. Evans, and D. J. O'Mahony. 2003. Peptidoglycan recognition protein expression in mouse Peyer's patch follicle associated epithelium suggests functional specialization. *Cell. Immunol.* 224: 8–16.
5. Hase, K., S. Ohshima, K. Kawano, N. Hashimoto, K. Matsumoto, H. Saito, and H. Ohno. 2005. Distinct gene expression profiles characterized cellular phenotypes of follicle-associated epithelium and M cells. *DNA Res.* 12: 127–137.
6. Verbrugghe, P., W. Waelput, B. Dieriks, A. Waeytens, J. Vandesompele, and C. A. Cuvelier. 2006. Murine M cells express annexin V specifically. *J. Pathol.* 209: 240–249.
7. Clark, M. A., M. A. Jepson, N. L. Simmons, T. A. Booth, and B. H. Hirst. 1993. Differential expression of lectin-binding sites defines mouse intestinal M-cells. *J. Histochem. Cytochem.* 41: 1679–1687.
8. Nochi, T., Y. Yuki, A. Matsumura, M. Mejima, K. Terahara, D. Y. Kim, S. Fukuyama, K. Iwatsuki-Horimoto, Y. Kawaoka, T. Kohda, et al. 2007. A novel M-cell-specific carbohydrate-targeted mucosal vaccine effectively induces antigen-specific immune responses. *J. Exp. Med.* 204: 2789–2796.
9. Jackson, R. J., K. Fujihashi, J. Xu-Amano, H. Kiyono, C. O. Elson, and J. R. McGhee. 1993. Optimizing oral vaccines: induction of systemic and mucosal B-cell and antibody responses to tetanus toxoid by use of cholera toxin as an adjuvant. *Infect. Immun.* 61: 4272–4279.
10. Xu-Amano, J., H. Kiyono, R. J. Jackson, H. F. Staats, K. Fujihashi, P. D. Burrows, C. O. Elson, S. Pillai, and J. R. McGhee. 1993. Helper T cell subsets for immunoglobulin A responses: oral immunization with tetanus toxoid and cholera toxin as adjuvant selectively induces Th2 cells in mucosa associated tissues. *J. Exp. Med.* 178: 1309–1320.
11. Yamamoto, M., K. Fujihashi, K. Kawabata, J. R. McGhee, and H. Kiyono. 1998. A mucosal intranet: intestinal epithelial cells down-regulate intraepithelial, but not peripheral, T lymphocytes. *J. Immunol.* 160: 2188–2196.
12. Yoshida, S., K. Ohbo, A. Takakura, H. Takebayashi, T. Okada, K. Abe, and Y. Nabeshima. 2001. Sgn1, a basic helix-loop-helix transcription factor delineates the salivary gland duct cell lineage in mice. *Dev. Biol.* 240: 517–530.
13. Zhao, X., A. Sato, C. S. Dela Cruz, M. Linehan, A. Luegering, T. Kucharzik, A. K. Shirakawa, G. Marquez, J. M. Farber, I. Williams, and A. Iwasaki. 2003. CCL9 is secreted by the follicle-associated epithelium and recruits dome region Peyer's patch CD11b$^+$ dendritic cells. *J. Immunol.* 171: 2797–2803.
14. Iwasaki, A., and B. L. Kelsall. 2000. Localization of distinct Peyer's patch dendritic cell subsets and their recruitment by chemokines macrophage inflammatory protein (MIP)-3α, MIP-3β, and secondary lymphoid organ chemokine. *J. Exp. Med.* 191: 1381–1393.
15. Cook, D. N., D. M. Prosser, R. Forster, J. Zhang, N. A. Kuklin, S. J. Abbondanzo, X. D. Niu, S. C. Chen, D. J. Manfra, M. T. Wiekowski, et al. 2000. CCR6 mediates dendritic cell localization, lymphocyte homeostasis, and immune responses in mucosal tissue. *Immunity* 12: 495–503.
16. Wang, X., I. Kochetkova, A. Haddad, T. Hoyt, D. M. Hone, and D. W. Pascual. 2005. Transgene vaccination using *Ulex europaeus* agglutinin I (UEA-1) for targeted mucosal immunization against HIV-1 envelope. *Vaccine* 23: 3836–3842.
17. Mays, R. W., K. A. Siemers, B. A. Fritz, A. W. Lowe, G. van Meer, and W. J. Nelson. 1995. Hierarchy of mechanisms involved in generating Na/K-ATPase polarity in MDCK epithelial cells. *J. Cell Biol.* 130: 1105–1115.
18. Aderem, A. 1992. The MARCKS brothers: a family of protein kinase C substrates. *Cell* 71: 713–716.
19. Blackshear, P. J. 1993. The MARCKS family of cellular protein kinase C substrates. *J. Biol. Chem.* 268: 1501–1504.
20. Zhu, Z., Z. Bao, and J. Li. 1995. MacMARCKS mutation blocks macrophage phagocytosis of zymosan. *J. Biol. Chem.* 270: 17652–17655.
21. Li, J., Z. Zhu, and Z. Bao. 1996. Role of MacMARCKS in integrin-dependent macrophage spreading and tyrosine phosphorylation of paxillin. *J. Biol. Chem.* 271: 12985–12990.
22. Underhill, D. M., J. Chen, L. A. H. Allen, and A. Aderem. 1998. MacMARCKS is not essential for phagocytosis in macrophages. *J. Biol. Chem.* 273: 33619–33623.
23. Clark, M. A., B. H. Hirst, and M. A. Jepson. 1998. M-cell surface β1 integrin expression and invasin-mediated targeting of *Yersinia pseudotuberculosis* to mouse Peyer's patch M cells. *Infect. Immun.* 66: 1237–1243.
24. Owen, R. L., and A. L. Jones. 1974. Epithelial cell specialization within human Peyer's patches: an ultrastructural study of intestinal lymphoid follicles. *Gastroenterology* 66: 189–203.
25. Hase, K., T. Murakami, H. Takatsu, T. Shimaoka, M. Iimura, K. Hamura, K. Kawano, S. Ohshima, R. Chihara, K. Itoh, et al. 2006. The membrane-bound chemokine CXCL16 expressed on follicle-associated epithelium and M cells mediates lympho-epithelial interaction in GALT. *J. Immunol.* 176: 43–51.
26. Matloubian, M., A. David, S. Engel, J. E. Ryan, and J. G. Cyster. 2000. A transmembrane CXC chemokine is a ligand for HIV-coreceptor Bonzo. *Nat. Immunol.* 1: 298–304.
27. Jahnsen, F. L., I. N. Farstad, J. P. Aanesen, and P. Brandtzaeg. 1998. Phenotypic distribution of T cells in human nasal mucosa differs from that in the gut. *Am. J. Respir. Cell Mol. Biol.* 18: 392–401.
28. Flach, C. F., S. Lange, E. Jennische, I. Lönnroth, and J. Holmgren. 2005. Cholera toxin induces a transient depletion of CD8$^+$ intraepithelial lymphocytes in the rat small intestine as detected by microarray and immunohistochemistry. *Infect. Immun.* 73: 5595–5602.
29. Leblond, C. P., and B. Messier. 1958. Renewal of chief cells and goblet cells in the small intestine as shown by radioautography after injection of thymidine-H3 into mice. *Anat. Rec.* 132: 247–259.
30. Borghesi, C., M. J. Taussig, and C. Nicoletti. 1999. Rapid appearance of M cells after microbial challenge is restricted at the periphery of the follicle-associated epithelium of Peyer's patch. *Lab. Invest.* 79: 1393–1401.
31. Lügering, A., M. Floer, N. Lügering, C. Cichon, M. A. Schmidt, W. Domschke, and T. Kucharzik. 2004. Characterization of M cell formation and associated mononuclear cells during indomethacin-induced intestinal inflammation. *Clin. Exp. Immunol.* 136: 232–238.

nature immunology

Regulation of humoral and cellular gut immunity by lamina propria dendritic cells expressing Toll-like receptor 5

Satoshi Uematsu[1,2,12], Kosuke Fujimoto[1,2,12], Myoung Ho Jang[3], Bo-Gie Yang[1], Yun-Jae Jung[4], Mika Nishiyama[5], Shintaro Sato[6], Tohru Tsujimura[7], Masafumi Yamamoto[8], Yoshifumi Yokota[9], Hiroshi Kiyono[6], Masayuki Miyasaka[5], Ken J Ishii[1,10,11] & Shizuo Akira[1,2,10]

The intestinal cell types responsible for defense against pathogenic organisms remain incompletely characterized. Here we identify a subset of CD11c^{hi}CD11b^{hi} lamina propria dendritic cells (LPDCs) that expressed Toll-like receptor 5 (TLR5) in the small intestine. When stimulated by the TLR5 ligand flagellin, TLR5$^+$ LPDCs induced the differentiation of naive B cells into immunoglobulin A–producing plasma cells by a mechanism independent of gut-associated lymphoid tissue. In addition, by a mechanism dependent on TLR5 stimulation, these LPDCs promoted the differentiation of antigen-specific interleukin 17–producing T helper cells and type 1 T helper cells. Unlike spleen DCs, the LPDCs specifically produced retinoic acid, which, in a dose-dependent way, supported the generation and retention of immunoglobulin A–producing cells in the lamina propria and positively regulated the differentiation interleukin 17–producing T helper cells. Our findings demonstrate unique properties of LPDCs and the importance of TLR5 for adaptive immunity in the intestine.

The gastrointestinal tract is constantly exposed to food proteins and commensal bacteria. Although the intestinal immune system has evolved mechanisms to maintain immunological tolerance to food and commensal organisms, it also recognizes invasive pathogens and properly induces protective immune responses to eliminate them. Dendritic cells (DCs) are thought to be critical in the 'decision' of whether to mount tolerant or protective immune responses[1]. Many subsets of DCs have been identified in the intestine[2]. In the Peyer's patches and mesenteric lymph nodes, conventional DCs consist of CD11c^{hi}CD11b$^+$CD8α^-, CD11c^{hi}CD11b$^-$CD8α^+ and CD11c^{hi}CD11b$^-$CD8α^- subsets[2]. In addition, there are CD11c^{int} plasmacytoid DCs in these sites[3,4]. Peyer's patch DCs produce interleukin 10 (IL-10) rather than IL-12, polarize naive T cells toward T helper type 2 (T_H2) or regulatory phenotypes[5] and induce the differentiation of plasma cells positive for immunoglobulin A (IgA)[6,7].

In contrast, lamina propria DCs (LPDCs) are less well studied. Although DCs are dominant antigen-presenting cells in the small intestine, colonic DCs are concentrated mainly in isolated lymphoid follicles, few of which are present in the lamina propria[8]. However, studies have shown that LPDCs of the small intestine and DCs in mesenteric lymph nodes that express CD103 have regulatory functions[9,10]. CD103$^+$ LPDCs migrate from the lamina propria to the mesenteric lymph nodes in a CCR7-dependent way[11–13] and promote the generation of Foxp3$^+$ regulatory T cells by means of retinoic acid[14]. Subsequent studies, however, have shown that CD11b$^+$F4/80$^+$CD11c$^-$ macrophages in the lamina propria are more potent inducers of regulatory T cells than are LPDCs and that CD11b$^+$ LPDCs generate T cells producing IL-17 *in vitro*[15]. These findings collectively suggest that LPDCs induce both 'tolerogenic' regulatory T cells and 'inflammatory' IL-17–producing T helper cells (T_H-17 cells). However, it remains unclear what kind of stimulation triggers the LPDC-induced generation of T_H-17 cells.

The Toll-like receptor (TLR) family, which is key for innate immunity, consists of 13 mammalian members[16]. TLRs are 'preferentially' expressed in 'professional' antigen-presenting cells such as DCs and macrophages and recognize specific components of

[1]Laboratory of Host Defense, Immunology Frontier Research Center, Osaka University, 3-1 Yamada-oka, Suita, Osaka 565-0871, Japan. [2]Department of Host Defense, Research Institute for Microbial Diseases, Osaka University, 3-1 Yamada-oka, Suita, Osaka 565-0871, Japan. [3]Laboratory of Gastrointestinal Immunology, Immunology Frontier Research Center, Osaka University, Suita, Osaka 565-0871, Japan. [4]Department of Microbiology, Gachon Medical School, Incheon 405-760, Korea. [5]Laboratory of Immunodynamics, Department of Microbiology and Immunology, Osaka University Graduate School of Medicine, Osaka 565-0871, Japan. [6]Division of Mucosal Immunology, Department of Microbiology and Immunology, The Institute of Medical Science, University of Tokyo, 108-8639 Tokyo, Japan. [7]Department of Pathology, Hyogo College of Medicine, 1, Mukogawa, Nishinomiya, Hyogo 663-8501, Japan. [8]Department of Microbiology and Immunology, Nihon University School of Dentistry at Matsudo, Chiba 271-8587, Japan. [9]Division of Molecular Genetics, School of Medicine, Faculty of Medical Sciences, University of Fukui, Fukui 910-1193, Japan. [10]Exploratory Research for Advanced Technology, Japan Science and Technology Corporation, 3-1 Yamada-oka, Suita, Osaka 565-0871, Japan. [11]Department of Molecular Protozoology, Research Institute for Microbial Diseases, Osaka University, 3-1 Yamada-oka, Suita, Osaka 565-0871, Japan. [12]These authors contributed equally to this work. Correspondence should be addressed to S.A. (sakira@biken.osaka-u.ac.jp).

Received 26 March; accepted 5 May; published online 30 May 2008; doi:10.1038/ni.1622

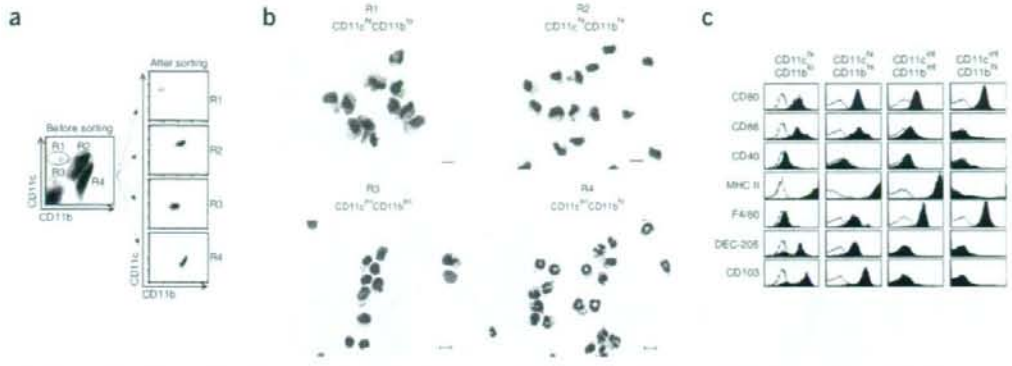

Figure 1 Four subsets of CD11c$^+$ LPCs in the small intestine. (**a**) Flow cytometry of intestinal low-density LPCs stained for CD11b and CD11c, before and after sorting. (**b**) May-Grunwald-Giemsa staining of four leukocyte subsets (gated in **a**) from the lamina propria. Scale bars, 10 μm. (**c**) Surface expression of CD80, CD86, CD40, major histocompatibility complex class II (MHC II), F4/80, DEC-205 and CD103 (filled histograms) on the four leukocyte subsets gated in **a**. Open histograms, isotype control. Data are representative of at least three independent experiments.

microorganisms to induce innate immune responses[16]. Each TLR activates specific signaling pathways that elicit biological responses to microorganisms, as well as DC maturation and cytokine production that shape adaptive immune responses[16]. Although the function of TLRs has been examined extensively in intestinal epithelial cells[17], the function of TLRs in lamina propria antigen-presenting cells has not been fully elucidated. Intestinal CD11c$^+$ lamina propria cells (LPCs) have high expression of TLR5 (A002297) and induce inflammatory responses when stimulated with the TLR5 ligand bacterial flagellin[18]. Unlike conventional DCs, such as those in the spleen (SPDCs), CD11c$^+$ LPCs do not express TLR4, which recognizes the Gram-negative bacterial component lipopolysaccharide (LPS)[18]. Nevertheless, *Tlr5*$^{-/-}$ mice show resistance to oral *Salmonella typhimurium* infection, as this facultative intracellular flagellated bacteria seems to use TLR5 and CD11c$^+$ LPCs as 'carriers' for systemic infection[18].

Mouse CD11c$^+$ LPCs consist of four subsets distinguished by differential expression patterns of CD11c and CD11b. Here we have identified a subset of CD11c^{hi}CD11b^{hi} LPDCs as TLR5-expressing cells. In response to flagellin, these LPDCs induced the differentiation of naive B cells into IgA$^+$ (A001174) plasma cells by a mechanism independent of gut-associated lymphoid tissue (GALT) and triggered the differentiation of antigen-specific T_H-17 and T_H1 cells. In a dose-dependent way, retinoic acid produced by LPDCs supported the generation and retention of IgA-producing cells in the lamina propria and positively regulated T_H-17 cell differentiation.

RESULTS

High TLR5 expression on CD11c^{hi}CD11b^{hi} LPDCs

CD11c$^+$ DCs constituted 10–15% of leukocytes in the small intestinal lamina propria and consisted of at least two subsets (CD11c^{hi}CD11b^{lo} (R1) and CD11c^{hi}CD11b^{hi} (R2))[12] (**Fig. 1a,b**), each of which had a DEC-205$^+$ major histocompatibility complex class II–high CD80$^+$CD86$^+$CD103$^+$ surface phenotype (**Fig. 1c**). In addition, CD11c^{hi}CD11b^{hi} cells had moderate expression of F4/80, which indicated a macrophage-like character. The remaining CD11c$^+$ subsets consisted of CD11c^{int}CD11b^{int} cells (R3), which are F4/80$^+$DEC-205$^-$ major histocompatibility complex class II$^+$ phagocytic macrophages[15,19], and CD11c^{int}CD11b^{hi} cells (R4), which are eosinophils with uniquely shaped nuclei and eosinophilic granules[12] (**Fig. 1b,c**). Of these four subsets from the lamina propria of C57BL/6 mice, only CD11c^{hi}CD11b^{hi} LPDCs expressed *Tlr5* mRNA (**Fig. 2a**). Consistent with the expression of functional TLR5, CD11c^{hi}CD11b^{hi} LPDCs produced proinflammatory cytokines such as IL-6, IL-12p40 and IL-12p70, but not IL-23 or IL-10, in response to flagellin (**Fig. 2b**). In contrast, LPDCs (R1) did not produce such cytokines in response to either flagellin or LPS (**Supplementary Fig. 1** online). Thus, CD11c^{hi}CD11b^{hi} LPDCs are responsible for TLR5-mediated innate immune responses.

CD11c^{hi}CD11b^{hi} LPDCs induce IgA production

To determine the function of CD11c^{hi}CD11b^{hi} LPDCs in adaptive immunity, we examined IgA synthesis in the small intestine. IgA is the

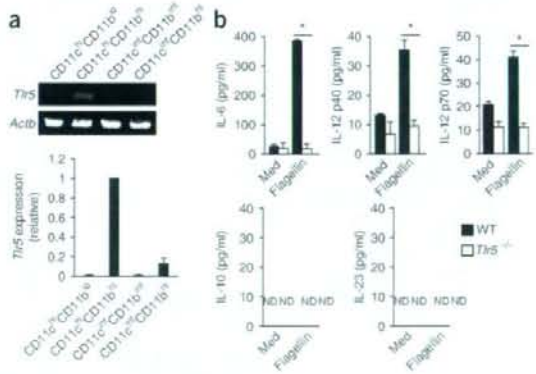

Figure 2 CD11c^{hi}CD11b^{hi} LPDCs specifically express TLR5. (**a**) RT-PCR (top) and quantitative real-time PCR (bottom) of *Tlr5* expression in the four leukocyte lamina propria subsets. *Actb* encodes β-actin (top, loading control). Expression (bottom) is relative to that of *Actb*. Data are representative of three independent experiments. (**b**) Cytokine production by CD11c^{hi}CD11b^{hi} LPDCs from wild-type (WT) and *Tlr5*$^{-/-}$ mice in response to medium alone (Med) or flagellin (1 μg/ml). ND, not detected. *, $P < 0.05$ (unpaired Student's *t*-test). Data represent the mean and s.d. of three independent experiments.

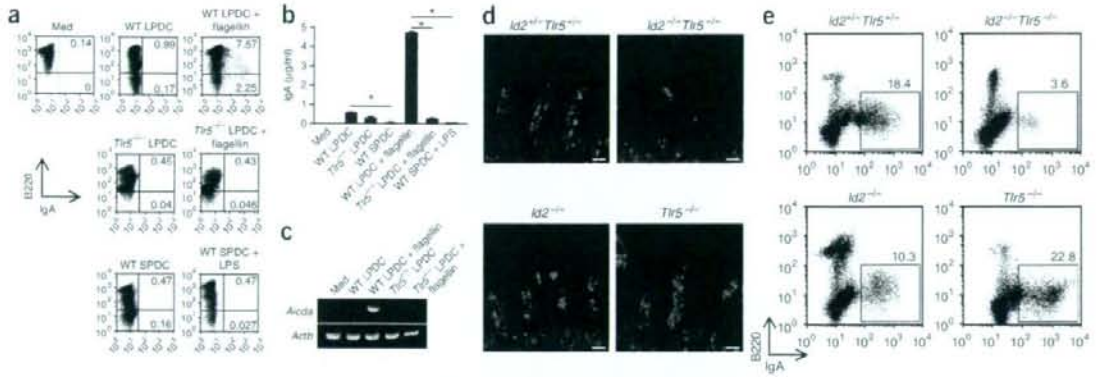

Figure 3 CD11c^{hi}CD11b^{hi} LPDCs induce IgA$^+$ plasma cell differentiation. (**a**,**b**) Flow cytometry (**a**) and ELISA (**b**) of peritoneal IgM$^+$IgD$^+$ cells cultured for 5 d in various conditions (above plots (**a**) and below horizontal axis (**b**)). (**a**) Cells stained for B220 and IgA (isotype controls, **Supplementary Fig. 2**). Numbers in quadrants indicate percent B220$^+$IgA$^+$ cells (top right) or B220$^-$IgA$^+$ cells (bottom right). Data are representative of three independent experiments. (**b**) Concentration of IgA in coculture supernatants. *, $P < 0.05$ (unpaired Student's *t*-test). Data represent the mean and s.d. of three independent experiments. (**c**) Expression of *Aicda* mRNA (encoding activation-induced cytidine deaminase) in IgM$^+$IgD$^+$ cells cultured together with wild-type or *Tlr5*$^{-/-}$ CD11c^{hi}CD11b^{hi} LPDCs with or without flagellin. Data are representative of three independent experiments. (**d**) Immunohistochemistry of IgA$^+$ cells (green) in the small intestine ($n = 4$ mice per group). Scale bars, 50 μm. Data are representative of three independent experiments. (**e**) Flow cytometry of LPCs stained for B220 and IgA. Numbers above outlined areas indicate percent B220$^-$IgA$^+$ cells. Data are representative of three independent experiments.

most abundant immunoglobulin in the gut[20]. Intestinal IgA$^+$ plasma cells are generated mainly in GALT, including Peyer's patches, isolated lymphoid follicles and mesenteric lymph nodes, by a mechanism dependent on antigen, T cells and the formation of germinal centers[21–23]. Differentiated IgA$^+$ cells are 'imprinted' by GALT DC–derived retinoic acid for gut homing through the selective expression of gut-homing receptors, including integrin $\alpha_4\beta_7$ and CCR9 (ref. 7). However, reports have shown that IgA$^+$ cell development does not necessarily require T cell help and the formation of germinal centers[21,24] and that GALT DC–derived retinoic acid can potently act in synergy with cytokines produced by DCs and/or other cells to generate T cell–independent IgA$^+$ cells[7]. Furthermore, it seems that some IgM$^+$ B cells, especially peritoneal B1 cells, migrate directly to the gut lamina propria by a mechanism dependent on sphingosine 1-phosphate[25,26] and differentiate into IgA$^+$ plasma cells in the lamina propria with the help of stroma cells[24]. Commensal bacteria induce natural secretory IgA, and this process is mediated by DCs loaded with commensal bacteria[6,27]. Nevertheless, although published work has suggested the involvement of DCs in gut IgA production[28,29], it is unknown what subset of DCs is responsible for this event and how this is achieved. We thus examined whether CD11c^{hi}CD11b^{hi} LPDCs are involved in the generation of IgA$^+$ cells; we used SPDCs (TLR5$^-$TLR4$^+$) for comparison[18]. Flagellin-stimulated CD11c^{hi}CD11b^{hi} LPDCs but not LPS-stimulated SPDCs efficiently induced the differentiation of B220$^-$ IgA$^+$ plasma cells in the absence of T cells in a TLR5-dependent way (**Fig. 3a,b** and **Supplementary Fig. 2** online). Expression of

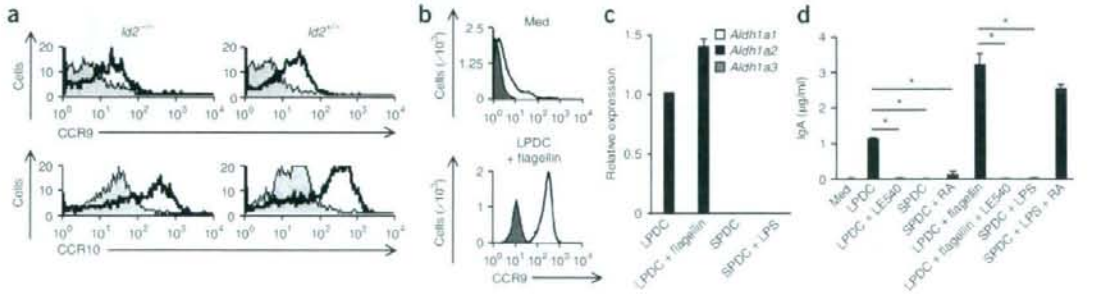

Figure 4 Function of retinoic acid released by CD11c^{hi}CD11b^{hi} LPDCs in IgA synthesis. (**a**) Flow cytometry of LPCs stained for B220, IgA, CCR9 or CCR10 (open histograms), gated on B220$^-$IgA$^+$ cells. Filled histograms, isotype control. Data are representative of three independent experiments. (**b**) Flow cytometry of peritoneal B220$^+$ cells cultured for 5 d with or without flagellin-stimulated CD11c^{hi}CD11b^{hi} LPDCs. Data for CCR9 (open histograms) were acquired after gating on B220$^+$ cells (top) or B220$^-$IgA$^+$ cells (bottom). Filled histograms, isotype control. Data are representative of three independent experiments. (**c**) Quantitative real-time PCR of mRNA encoding retinal dehydrogenase isozymes (key) in CD11c^{hi}CD11b^{hi} LPDCs and SPDCs left unstimulated or stimulated with LPS or flagellin (horizontal axis). Data are representative of three independent experiments (mean and s.d.). (**d**) ELISA of IgA in supernatants of peritoneal B220$^+$ cells cultured for 5 d in various conditions (horizontal axis) with or without LE540 (1 μM) or retinoic acid (RA; 1 nM). *, $P < 0.05$ (unpaired Student's *t*-test). Data represent the mean and s.d. of three independent experiments.

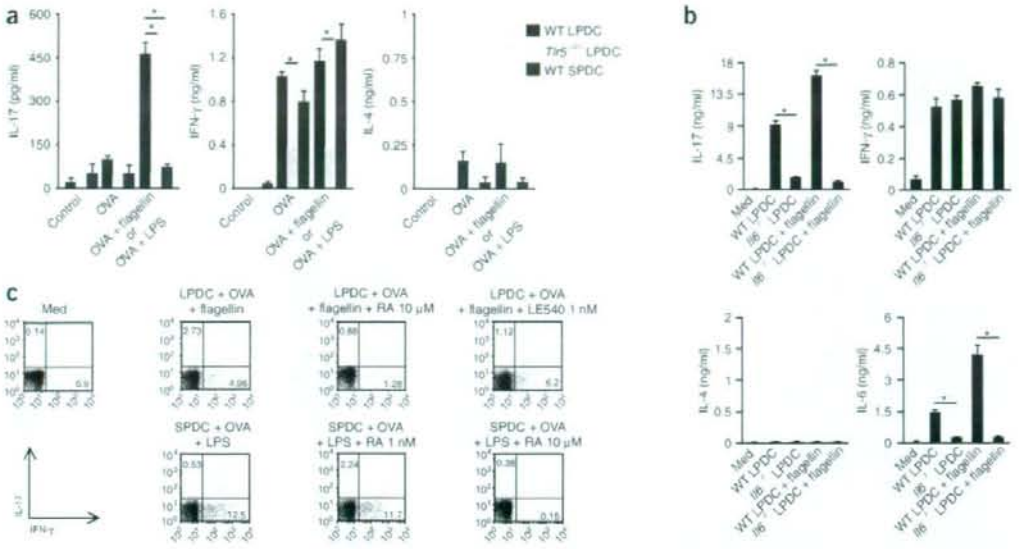

Figure 5 TLR5-dependent T_H-17 cell differentiation by $CD11c^{hi}CD11b^{hi}$ LPDCs. (**a**) ELISA of IFN-γ, IL-17 and IL-4 in culture supernatants. $CD11c^{hi}CD11b^{hi}$ LPDCs or SPDCs cultured for 12 h with OVA protein (100 μg/ml) in the presence or absence of flagellin (1 μg/ml) or LPS (1 μg/ml) were injected on days 0 and 14 into the peritoneal cavities of naive *Tlr5*$^{-/-}$ mice (wild-type $CD11c^{hi}CD11b^{hi}$ LPDCs) or *Tlr4*$^{-/-}$ mice (wild-type SPDCs) at a dose of 5×10^4 antigen-loaded cells per mouse; control mice were treated with PBS. At 1 week after the final immunization, splenocytes were collected and were cultured for 4 d with OVA protein (10 μg/ml) or with OVA peptide (amino acids 323–339; 10 μg/ml; **Supplementary Fig. 6**). *, $P < 0.05$ (unpaired Student's *t*-test). Data represent the mean and s.d. of three independent experiments. (**b**) ELISA of cytokines in supernatants of OT-II transgenic $CD4^+$ T cells cultured for 4 d together with wild-type or *Il6*$^{-/-}$ $CD11c^{hi}CD11b^{hi}$ LPDCs (conditions, horizontal axes). *, $P < 0.05$ (unpaired Student's *t*-test). Data represent the mean and s.d. of three independent experiments. (**c**) Flow cytometry of OT-II transgenic $CD4^+$ T cells cultured for 4 d in various conditions (above plots) and stained intracellularly for IL-17 and IFN-γ (isotype controls, **Supplementary Fig. 7a**). Numbers in quadrants indicate percent $IL\text{-}17^+IFN\text{-}\gamma^-$ cells (top left) or $IL\text{-}17^-IFN\text{-}\gamma^+$ cells (bottom right). Data are representative of three independent experiments.

mRNA encoding activation-induced cytidine deaminase[30], an enzyme essential for class-switch recombination, was upregulated in naive B cells cultured together with flagellin-stimulated $CD11c^{hi}CD11b^{hi}$ LPDCs (**Fig. 3c**).

Although the results presented above demonstrated that $CD11c^{hi}$ $CD11b^{hi}$ LPDCs were able to induce T cell–independent differentiation of IgA^+ cells *in vitro*, we also examined the *in vivo* function of TLR5 in IgA synthesis by using GALT-deficient mice that intrinsically lack secondary lymphoid organs but have LPDCs. Mice lacking the transcription factors Id2 or RORγt, as well as bone marrow–reconstituted mice lacking lymphotoxin-α or both lymphotoxin-α and tumor necrosis factor, do not develop GALT, yet they retain intestinal IgA production[21,31]. Indeed, we detected many IgA^+ cells in the lamina propria of *Id2*$^{-/-}$ mice, which confirmed that gut IgA can be generated without GALT (**Fig. 3d,e**). Furthermore, we found no defects in the *in vitro* differentiation of IgA^+ plasma cells induced by $CD11c^{hi}$ $CD11b^{hi}$ LPDCs from peritoneal B cells isolated from *Id2*$^{-/-}$ mice (**Supplementary Fig. 3** online). Although *Tlr5*$^{-/-}$ mice did not have fewer IgA^+ B cells, *Id2*$^{-/-}$*Tlr5*$^{-/-}$ mice had far fewer IgA^+ cells in the lamina propria (**Fig. 3d,e**). Thus, TLR5 signaling in $CD11c^{hi}CD11b^{hi}$ LPDCs is critical for GALT-independent IgA synthesis *in vivo*.

Retinoic acid in LPDC-induced IgA synthesis

We next examined the expression of gut-homing receptors on lamina propria IgA^+ cells in *Id2*$^{-/-}$ mice. Unexpectedly, $B220^-IgA^+$ plasma cells in the lamina propria of *Id2*$^{-/-}$ mice had high expression of CCR9, despite the lack of GALT in these mice (**Fig. 4a**). These cells also expressed CCR10, another chemokine receptor important for gut tropism[32]. As we did not detect high CCR9 expression on either peritoneal or splenic unstimulated $B220^+$ cells from wild-type or *Id2*$^{-/-}$ mice (**Fig. 4b** and data not shown), CCR9 might be induced on B cells only after their migration to the lamina propria in *Id2*$^{-/-}$ mice. In contrast, coculture with flagellin-treated $CD11c^{hi}CD11b^{hi}$ LPDCs induced CCR9 expression on peritoneal $B220^-IgA^+$ cells (**Fig. 4b**). We therefore determined whether $CD11c^{hi}CD11b^{hi}$ LPDCs synthesize retinoic acid, a mediator able to induce CCR9 expression. Retinal is converted into retinoic acid by retinal dehydrogenase enzymes. Although we detected no mRNA molecules encoding retinal dehydrogenase isoforms in SPDCs, $CD11c^{hi}CD11b^{hi}$ LPDCs specifically expressed *Aldh1a2* mRNA, which encodes retinal dehydrogenase 2 (**Fig. 4c**). To determine if the $CD11c^{hi}CD11b^{hi}$ LPDC–mediated development of IgA^+ cells was controlled by retinoic acid, we added the retinoic acid receptor inhibitor LE540 during the *in vitro* coculture of B cells and $CD11c^{hi}CD11b^{hi}$ LPDCs. LE540 abrogated IgA production by B cells cultured together with flagellin-activated $CD11c^{hi}CD11b^{hi}$ LPDCs (**Fig. 4d**). Moreover, supplementation of LPS-activated SPDCs with retinoic acid increased IgA concentrations to an extent similar to that induced by flagellin-activated $CD11c^{hi}CD11b^{hi}$ LPDCs. Thus, the characteristic ability to synthesize retinoic acid grants $CD11c^{hi}CD11b^{hi}$ LPDCs the ability to generate T cell–independent IgA^+ cells.

LPDC-induced T_H-17 cell differentiation

We next assessed the ability of $CD11c^{hi}CD11b^{hi}$ LPDCs to induce antigen-specific T helper cell differentiation of ovalubumin

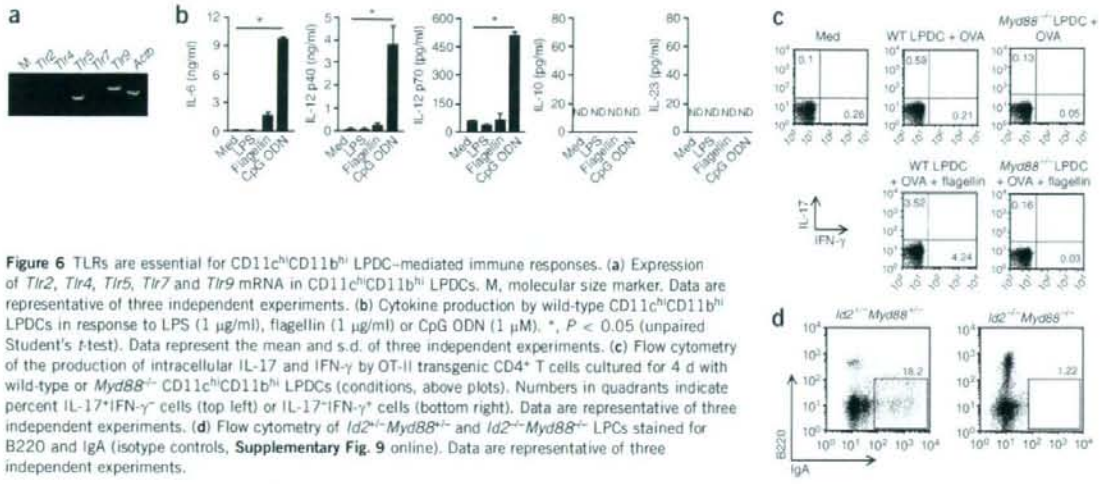

Figure 6 TLRs are essential for $CD11c^{hi}CD11b^{hi}$ LPDC–mediated immune responses. (**a**) Expression of *Tlr2*, *Tlr4*, *Tlr5*, *Tlr7* and *Tlr9* mRNA in $CD11c^{hi}CD11b^{hi}$ LPDCs. M, molecular size marker. Data are representative of three independent experiments. (**b**) Cytokine production by wild-type $CD11c^{hi}CD11b^{hi}$ LPDCs in response to LPS (1 μg/ml), flagellin (1 μg/ml) or CpG ODN (1 μM). *, $P < 0.05$ (unpaired Student's *t*-test). Data represent the mean and s.d. of three independent experiments. (**c**) Flow cytometry of the production of intracellular IL-17 and IFN-γ by OT-II transgenic $CD4^+$ T cells cultured for 4 d with wild-type or *Myd88*$^{-/-}$ $CD11c^{hi}CD11b^{hi}$ LPDCs (conditions, above plots). Numbers in quadrants indicate percent $IL\text{-}17^+IFN\text{-}\gamma^-$ cells (top left) or $IL\text{-}17^+IFN\text{-}\gamma^+$ cells (bottom right). Data are representative of three independent experiments. (**d**) Flow cytometry of *Id2*$^{+/-}$*Myd88*$^{+/-}$ and *Id2*$^{-/-}$*Myd88*$^{+/-}$ LPCs stained for B220 and IgA (isotype controls, **Supplementary Fig. 9** online). Data are representative of three independent experiments.

(OVA)-specific OT-II-transgenic $CD4^+$ T cells. Although we detected only interferon-γ (IFN-γ)-producing cells in cocultures of OT-II T cells and LPS-stimulated SPDCs, we detected both IL-17- and IFN-γ-producing cells in cocultures of OT-II T cells and $CD11c^{hi}CD11b^{hi}$ LPDCs; the numbers of IL-17- and IFN-γ-producing OT-II cells were further increased by flagellin stimulation of LPDCs[33–36] (**Supplementary Fig. 4a,b** online). In support of the idea that $TLR5^+$ $CD11c^{hi}CD11b^{hi}$ LPDCs induce T_H-17 differentiation, naive $CD4^+$ T cells cultured together with wild-type $CD11c^{hi}CD11b^{hi}$ LPDCs had higher expression of RORγt and IL-21, but those cultured together with *Tlr5*$^{-/-}$ $CD11c^{hi}CD11b^{hi}$ LPDCs did not (**Supplementary Fig. 4c,d**). In contrast, other LPDC subsets (R1, R3 and R4) induced neither IL-17 nor IFN-γ production in response to flagellin (**Supplementary Fig. 5** online).

Next we examined *in vivo* the T helper cell responses of mice immunized with antigen-loaded DCs. We detected antigen-specific IFN-γ production after injection of both SPDCs and $CD11c^{hi}CD11b^{hi}$ LPDCs, and this production was augmented by stimulation of TLR5 and TLR4 (**Fig. 5a** and **Supplementary Fig. 6** online). In addition, large amounts of IL-17 were produced by splenocytes from mice injected with flagellin-stimulated $CD11c^{hi}CD11b^{hi}$ LPDCs but not those injected with LPS-stimulated SPDCs. Those responses were impaired when mice were injected with *Tlr5*$^{-/-}$ $CD11c^{hi}CD11b^{hi}$ LPDCs. As IL-6 is an essential cytokine for T_H-17 cell differentiation, and as $CD11c^{hi}CD11b^{hi}$ LPDCs produced IL-6 in response to TLR5 stimulation (**Fig. 2b**), we then examined the involvement of IL-6 in $CD11c^{hi}CD11b^{hi}$ LPDCs–induced T_H-17 cell differentiation[37]. Despite normal induction of IFN-γ, IL-17 production induced by flagellin-stimulated *Il6*$^{-/-}$ $CD11c^{hi}CD11b^{hi}$ LPDCs was significantly lower than that elicited by flagellin-stimulated wild-type $CD11c^{hi}CD11b^{hi}$ LPDCs (**Fig. 5b**).

A series of studies has shown that retinoic acid negatively regulates T_H-17 cell differentiation[38–40]. In agreement with those results, supplementation of cocultures of T cells and $CD11c^{hi}CD11b^{hi}$ LPDCs with 10 μM retinoic acid effectively inhibited *in vitro* T_H-17 cell differentiation; retinoic acid supplementation also suppressed T_H1 cell differentiation (**Fig. 5c** and **Supplementary Fig. 7** online). However, we suspected that this concentration of retinoic acid may have been too high, as plasma retinoic acid concentrations are usually on the order of 10 nM and retinoic acid efficiently enhances the expression of gut-homing receptors on $CD8^+$ T cells even at a concentration of 0.1 nM (ref. 41). Notably, the retinoic acid inhibitor LE540 inhibited the differentiation of T_H-17 cells but not T_H1 cells, which suggested that retinoic acid from $CD11c^{hi}CD11b^{hi}$ LPDCs is actually necessary for T_H-17 cell differentiation. In line with that observation, LPS-stimulated SPDCs induced T_H-17 cell differentiation to the same extent as flagellin-stimulated $CD11c^{hi}CD11b^{hi}$ LPDCs when cultured together with 1 nM retinoic acid, and 10 μM retinoic acid abolished T_H1 cell differentiation induced by LPS-stimulated SPDCs (**Fig. 5c** and **Supplementary Fig. 7**). Thus, retinoic acid at a low concentration acts as a positive regulator of T_H-17 cell differentiation, and the effect of retinoic acid on T_H-17 cell differentiation depends on its concentration.

$CD11c^{hi}CD11b^{hi}$ LPDCs induce antigen-specific T_H-17 cells and T_H1 cells, but it is not clear whether these adaptive immune responses are protective against bacterial infection. T_H-17 cells constitute approximately 2% of the total $CD4^+$ T cell population in the small intestinal lamina propria of C57BL/6 mice without infection, and the number of T_H-17 cells did not change during the acute phase of oral *S. typhimurium* infection (**Supplementary Fig. 8a** online). Mice immunized with OVA-loaded $CD11c^{hi}CD11b^{hi}$ LPDCs had greater proportions of T_H-17 and T_H1 cells in the lamina propria (**Supplementary Fig. 8b**). Challenge of the immunized mice with oral OVA further increased the proportions of lamina propria T_H-17 and T_H1 cells. Similarly, immunization with *S. typhimurium* flagellin–loaded wild-type LPDCs resulted in a significant increase in the proportion of lamina propria T_H-17 cells after oral challenge with *S. typhimurium*, ($P < 0.05$; **Supplementary Fig. 8c**) and resulted in partial protection against lethal challenge with *S. typhimurium* (**Supplementary Fig. 8d**), but similar immunization with *Tlr5*$^{-/-}$ LPDCs did not. Thus, $CD11c^{hi}CD11b^{hi}$ LPDC–mediated immunization contributed to host defense against *S. typhimurium*.

TLR signals in LPDC-mediated inflammation

Although we demonstrated the importance of TLR5 in the activation of adaptive immunity by $CD11c^{hi}CD11b^{hi}$ LPDCs, *Tlr5*$^{-/-}$ $CD11c^{hi}CD11b^{hi}$ LPDCs nevertheless induced small amounts of IL-17- and IFN-γ-producing cells (**Supplementary Fig. 4a**). In

addition, we detected residual B220$^-$IgA$^+$ plasma cells in the lamina propria of *Id2*$^{-/-}$*Tlr5*$^{-/-}$ mice (**Fig. 3e**). Thus, other TLRs may contribute to such responses. Accordingly, CD11c^{hi}CD11b^{hi} LPDCs expressed TLR9 as well as TLR5 and produced proinflammatory cytokines in response to the TLR9 ligand CpG DNA (**Fig. 6a,b**). Notably, unlike wild-type CD11c^{hi}CD11b^{hi} LPDCs, *Myd88*$^{-/-}$ CD11c^{hi}CD11b^{hi} LPDCs failed to induce the *in vitro* differentiation of T_H-17 and T_H1 cells (**Fig. 6c**). Furthermore, B220$^-$IgA$^+$ cells were almost completely absent from the lamina propria of *Id2*$^{-/-}$*Myd88*$^{-/-}$ mice (**Fig. 6d**). These data collectively suggest that TLR signals in general are critical for CD11c^{hi}CD11b^{hi} LPDC–mediated activation of acquired immunity.

DISCUSSION

In this work we have demonstrated the unique characteristics of CD11c^{hi}CD11b^{hi} TLR5-expressing LPDCs. It is noteworthy that TLR5 activation by flagellin triggered CD11c^{hi}CD11b^{hi} LPDC–mediated adaptive immune responses. Studies have shown that adjuvant effects are associated with the induction of protective immunity in the intestine. Injection of the ligand for the receptor tyrosine kinase Flt3, which expands DC populations in the intestine, enhances both tolerance and immunity to orally administered antigens[42,43]. Relative to mice fed antigen alone, those receiving Flt3 ligand and antigen show greater susceptibility to the induction of oral tolerance[42]. However, such oral tolerance is abrogated and immune responses are induced when mice are fed the same antigen with an adjuvant such as IL-1 or cholera toxin[43]. Such findings indicate that DC activation is a crucial parameter determining whether tolerance or protective immunity is induced in the intestine. In physiological conditions, antigens such as food proteins may be presented by quiescent CD11c^{hi}CD11b^{hi} LPDCs in the absence of inflammation, leading to tolerance. However, when inflammatory stimuli such as flagellin are present, CD11c^{hi}CD11b^{hi} LPDCs will undergo maturation, release inflammatory cytokines and initiate protective acquired immunity.

Commensal bacteria are present at a high density in the intestinal lumen (up to 1×10^{12} bacteria per gram of lumenal contents). Most commensal organisms reside outside the layer of mucus that covers the intestinal epithelial cells. Some bacteria penetrate the enterocyte epithelial layer but are rapidly killed by macrophages[44]. However, some commensal bacteria are ingested by DCs, where they survive for several days[6]. Moreover, intraepithelial DCs send protrusions into the lumen of the small intestine in a CX3CR1-dependent way and directly sample lumenal commensal bacteria[45,46]. Commensal bacteria–loaded DCs mediate the induction of natural secretary IgA[27], and germ-free mice have a profound deficiency in IgA production in the intestinal mucosa[44]. Thus, the presence of intestinal microbiota influences IgA production in the intestine. As the induction of B220$^-$IgA$^+$ plasma cells was impaired in *Id2*$^{-/-}$*Tlr5*$^{-/-}$ mice and was almost completely abrogated in *Id2*$^{-/-}$*Myd88*$^{-/-}$ mice, GALT-independent IgA production seems to be mediated by TLR stimulation. These results indicate that TLRs represent a 'missing link' between commensal bacteria and IgA synthesis in the lamina propria.

The ability to synthesize retinoic acid enables CD11c^{hi}CD11b^{hi} LPDCs to modulate various immune response parameters. CD11c^{hi}CD11b^{hi} LPDCs induced IgA$^+$ cell differentiation without T cell help in a retinoic acid–dependent way. In the process, CD11c^{hi}CD11b^{hi} LPDCs also promoted the upregulation of CCR9 expression on B cells. Notably, IgA$^+$ plasma cells had high expression CCR9 in the lamina propria of GALT-deficient *Id2*$^{-/-}$ mice. These results were unexpected, because GALT DCs are believed to 'imprint' gut tropism on lymphocytes. The ability of CD11c^{hi}CD11b^{hi} LPDCs to induce CCR9 on differentiated IgA$^+$ plasma cells may promote retention in the lamina propria, as the CCR9 ligand CCL25 is abundantly secreted by the crypt epithelium[21]. Although previous studies have shown that retinoic acid negatively regulates T_H-17 cell differentiation, here we have shown that the effect of retinoic acid on T helper cell differentiation depended strictly on its concentration. It is difficult to determine the local concentrations of retinoic acid secreted by CD11c^{hi}CD11b^{hi} LPDCs. However, studies intensively examining the concentration of retinoic acid secreted by GALT DCs in the work of T cell 'imprinting' have shown that 1 nM of retinoic acid is the optimum concentration for the induction of gut-homing receptors on T cells[41]. Notably, high concentrations of retinoic acid inhibited the differentiation of both T_H1 and T_H-17 cells, which suggested that the inhibitory effect of high concentrations of retinoic acid is not specific for T_H-17 polarization. Such observations indicate that the effect of retinoic acid on T_H-17 cell differentiation should be considered more cautiously. In any case, like the CD11c^{hi}CD11b^{hi} LPDC–induced differentiation of IgA$^+$ plasma cells, T_H-17 cell differentiation required retinoic acid. Unlike other conventional DCs, LPDCs can induce the differentiation of antigen-specific T_H-17 cells as well as T_H1 cells in response to TLR stimulation. The ability to produce retinoic acid may support this unique function of CD11c^{hi}CD11b^{hi} LPDCs.

We conclude that CD11c^{hi}CD11b^{hi} LPDCs may work against bacterial infection by inducing 'local' IgA secretion and 'systemic' T helper cell responses through TLR stimulation. As IL-17 can influence cytokine production by a wide range of cell types and can induce the activation and migration of neutrophils[47], CD11c^{hi}CD11b^{hi} LPDCs and T_H-17 cells may modulate the pathogenesis of intestinal bowel diseases such as Crohn's disease. In addition, the ability of CD11c^{hi}CD11b^{hi} LPDCs to induce the differentiation of T_H1 and IgA$^+$ cells suggests that CD11c^{hi}CD11b^{hi} LPDCs might be useful targets of mucosal vaccination.

METHODS

Mice. *Tlr4*$^{-/-}$ (C57BL/6) mice, *Tlr5*$^{-/-}$ mice (C57BL/6), *Id2*$^{-/-}$ mice and *Myd88*$^{-/-}$ mice have been described[18,48]. *Il6*$^{-/-}$ mice (C57BL/6) and OT-II-transgenic mice (C57BL/6) were provided by M. Kopf[49] and W.R. Heath[50], respectively. All animal experiments were done with the approval of the Animal Research Committee of the Research Institute for Microbial Diseases at Osaka University.

Reagents. LPS, flagellin and CpG oligodeoxynucleotides (ODN 1668) were purified as described[18]. *S. typhimurium* flagellin was from Invivogen. All-*trans* retinoic acid (Sigma) was dissolved in dimethyl sulfoxide, was stored at −80 °C with light interception and was added to cultures at a final concentration of 1 nM. LE540 (Wako) was dissolved in dimethyl sulfoxide and was added to cultures at a final concentration of 1 μM.

Cells. Segments of the small intestine were treated for 30 min at 37 °C with PBS containing 10% (vol/vol) FCS, HEPES (20 mM), pH 7.4, penicillin (100 U/ml), streptomycin (100 μg/ml), sodium pyruvate (1 mM), EDTA (10 mM) and polymyxin B (10 μg/ml; Calbiochem) for removal of epithelial cells, then were washed extensively with PBS. Segments of the small intestine and spleen were digested for 45–90 min with continuous stirring at 37 °C with collagenase D (400 Mandl units/ml; Roche) and DNase I (10 μg/ml; Roche) in RPMI 1640 medium plus 10% (vol/vol) FCS. EDTA was added (final concentration, 10 mM) and cell suspensions were incubated for an additional 5 min at 37 °C. Cells were spun through a 17.5% (wt/vol) solution of Accudenz (Accurate Chemical & Scientific) for enrichment for DCs. The cells obtained were incubated with fluorescein isothiocyanate–conjugated antibody to CD11b (anti-CD11b; M170; 557396) and phycoerythrin-conjugated anti-CD11c (HL3; 557401; both from BD Pharmingen) after blockade of Fc receptors. DC subsets were sorted on the basis of their expression of CD11c and CD11b with a FACSVantage SE or FACSAria (BD Biosciences). The purity of the sorted DCs

was routinely over 95%. For morphological studies, cytospin preparations from purified DC subsets were stained with May-Grunwald-Giemsa solution. For analysis of leukocytes, cells were subjected to density-gradient centrifugation in 40% to 75% (vol/vol) Percoll (approximately density, 1.058 g/ml and 1.093 g/ml, respectively) after enzyme treatment. Cells collected from the interface were washed and were used as lamina propria leukocytes in assays. Naive $CD4^+$ T cells from the spleens of OT-II transgenic mice and $B220^+$ cells from the peritoneal cavities of C57BL/6 mice were purified by magnetic sorting with mouse anti-CD4 beads and mouse anti-B220 beads, respectively. Peritoneal cells from C57BL/6 mice were incubated with fluorescein isothiocyanate–conjugated conjugated anti-IgD (11-26c.2a; 553439; BD Pharmingen) and phycoerythrin-indotricarbocyanine–conjugated anti-IgM (R6-60.2; 553409; BD Pharmingen) after blockade of Fc receptors. Naive B cells were sorted on the basis of their expression of IgD and IgM with a FACSVantage SEM or FACSAria (BD Biosciences). The purity of the sorted cells was routinely over 95%.

***In vitro* T cell differentiation.** OT-II transgenic $CD4^+$ T cells (1×10^6) were cultured with $CD11c^{hi}CD11b^{hi}$ LPDCs or SPDCs (1×10^5) in the presence of OVA protein (100 μg/ml), unsupplemented or supplemented with flagellin (1μg/ml) or LPS (1 μg/ml), respectively. After 4 d, cells were restimulated for 4 h with phorbol 12-myristate 13-acetate (50 ng/ml; Sigma) and ionomycin (500 ng/ml; Calbiochem) in the presence of GolgiStop (BD Pharmingen), then cells producing IL-17 and IFN-γ were analyzed by flow cytometry.

Immunization. $CD11c^{hi}CD11b^{hi}$ LPDCs or SPDCs were cultured for 12 h with OVA protein (100 μg/ml) in the presence or absence of flagellin (1 μg/ml) or LPS (1 μg/ml). Antigen-loading cells (5×10^4 per mouse) were injected on days 0 and 14 into the peritoneal cavities of naive *Tlr5*$^{-/-}$ mice ($CD11c^{hi}CD11b^{hi}$ LPDCs) or *Tlr4*$^{-/-}$ mice (SPDCs); control mice were treated with PBS. At 1 week after the final immunization, splenocytes were collected and were cultured for 4 d with OVA protein (10 μg/ml). The concentration of IFN-γ, IL-17 and IL-4 in the culture supernatants was measured by enzyme-linked immunosorbent assay (ELISA).

***In vitro* IgA^+ plasma cell differentiation.** Peritoneal IgM^+IgD^+ cells or $B220^+$ cells (1×10^6) were cultured in medium supplemented with B cell–activating factor (50 ng/ml) together with $CD11c^{hi}CD11b^{hi}$ LPDCs or SPDCs (1×10^5 to 5×10^5) in the presence or absence of flagellin (1 μg/ml) or LPS (1 μg/ml), respectively. After 5 d, cells were analyzed by flow cytometry and the concentration of IgA in culture supernatants was measured by ELISA.

Flow cytometry. Before staining, Fc receptors were blocked for 15 min at 4 °C. Low-density LPCs were stained with the following biotinylated monoclonal antibodies: anti-CD11b (M1/70; 557395), anti-CD11c (HL3; 553800), anti-CD40 (3/23; 553789), anti-CD80 (16-10A1; 553767), anti-CD86 (GL1; 553690), anti-I-A/I-E (2G9; 553622) and anti-CD103 (M290; 557493; all from BD Pharmingen); anti-F4/80 (A3-1; MF48015; Caltag Laboratories); and anti-DEC-205 (NLDC-145; CL89145PE; Cedarlane Laboratories). The surfaces of cocultured T cells were stained with fluorescein isothiocyanate–labeled anti-CD4 (L3T4; 553055; BD Pharmingen). Then, cells were fixed and made permeable with Cytofix/Cytoperm (BD Pharmingen) and were stained intracellularly with phycoerythrin-labeled anti-IL-17 (TCC11-18H10.1; 559502) and allophycocyanin-labeled anti-IFN-γ (XMG1.2; 554413; both from BD Pharmingen). The surfaces of cocultured B cells or lamina propria leukocytes were stained with phycoerythrin-labeled anti-B220 (RA3-6B2; 553090; BD Pharmingen). Then, cells were fixed and made permeable with Cytofix/Cytoperm and were stained intracellularly with fluorescein isothiocyanate–labeled anti-IgA (C10-3; 559354) or were incubated with biotin-conjugated IgA (C10-1; 556978) and then stained intracellulary with allophycocyanin-labeled streptavidin (all from BD Pharmingen). CCR9 expression on lamina propria leukocytes and cocultured B cells was assessed with rat anti–mouse CCR9 (242503; FAB2160A; R&D Systems). CCR10 expression on lamina propria leukocytes and cocultured B cells was assessed with rat anti-mouse CCR10 (248918; FAB2815A; R&D Systems). Samples were acquired on a FACSCalibur with CELLQuest software (BD Biosciences) and data were analyzed with FlowJo software (TreeStar).

RT-PCR and quantitative real-time PCR. RNA (1 μg) was reverse-transcribed with Superscript2 (Invitrogen) according to the manufacturer's instructions with random hexamers as primers. Primer pairs specific for *Tlr2*, *Tlr4*, *Tlr5*, *Tlr7*, *Tlr9*, *Aicda*[30] or *Actb* (**Supplementary Table 1** online) and Taq polymerase[18] (Takara Shuzo) were used for PCR of 25 cycles at 97 °C for 30 s, 57 °C for 30 s and 72 °C for 30 s; products were separated by agarose gel electrophoresis. A 7700 Sequence Detector (Applied Biosystems) was used for quantitative real-time PCR of cDNA amplified as described above with 2× PCR Master Mix (Applied Biosystems) and primers for 18S rRNA (as an internal control; Applied Biosystems) or primers specific for *Tlr5*, *Rorc*, *Aldh1a1*, *Aldh1a2* or *Aldh1a3* (Applied Biosystems), in a final volume of 25 μl. After incubation at 95 °C for 10 min, products were amplified by 35 cycles of 95 °C for 15 s, 60 °C for 60 s and 50 °C for 120 s.

Measurement of cytokines in supernatants. The concentrations of IFN-γ, IL-17, IL-4, IL-6, IL-10 and IL-12p40 were measured with the Bio-plex system (Bio-Rad) according to the manufacturer's instructions. The concentrations of IL-21, IL-23 and IgA were determined by ELISA (R&D Systems, eBioscience and Southern Biotech, respectively).

Immunohistochemical analysis. For analysis of the number of IgA^+ cells in the small intestinal lamina propria, fluorescein isothiocyanate–conjugated anti–mouse IgA (C10-3; 559354; BD Pharmingen) was applied overnight at 4 °C to sections cut from frozen tissue. Immunohistochemical staining was analyzed with a Radiance 2100 Bio-Rad confocal laser microscope (Bio-Rad).

Bacterial infection. *S. enterica* serovar *typhimurium* has been described[18]. *S. typhimurium* was grown in Luria-Bertani medium without shaking at 37 °C. The concentration of bacteria was determined on the basis of the absorbance at 600 nm. Bacteria were injected orally into mice.

Statistical analysis. Statistical significance was evaluated with an unpaired two-tailed Student's *t*-test in all experiments except **Supplementary Figure 8d**. A P value of less than 0.05 was considered significant. Kaplan-Meier plots and log-rank tests were used to assess the survival differences of control and mutant mice after bacterial infection (**Supplementary Fig. 8d**).

Accession codes. UCSD-Nature Signaling Gateway (http://www.signaling-gateway.org/): A002297 and A001174.

Note: Supplementary information is available on the Nature Immunology website.

ACKNOWLEDGMENTS

We thank N. Kitagaki for technical assistance; T. Kawai and C. Coban for discussions; and A. Shigeta and M. Matsumoto for the distribution of OT-II-transgenic mice. *Il6*$^{-/-}$ mice (C57BL/6) were provided by M. Kopf (Swiss Federal Institute of Technology), and OT-II transgenic mice (C57BL/6) were provided by W.R. Heath (The Walter and Eliza Hall Institute of Medical Research). Supported by the Ministry of Education, Culture, Sports, Science and Technology in Japan (S.A.), the Ministry of Health, Labour and Welfare in Japan (S.A.), the 21st Century Center of Excellence Program of Japan (S.A.), the World Premier International Research Center (S.A.) and the National Institutes of Health (AI070167 to S.A.).

AUTHOR CONTRIBUTIONS

K.F. and S.U. did most of the experiments; S.U., K.J.I. and M.H.I. designed all the experiments; B.-G.Y. helped with the immunohistochemical analysis; Y.-I.I. and M.N. helped to isolate cells; S.S., T.T. and M.Y. provided advice for the experiments; Y.Y. provided *Id2*$^{-/-}$ mice; H.K. and M.M. provided advice for the experiments and manuscript; S.U. and S.A. prepared the manuscript; and S.A. directed the research.

Published online at http://www.nature.com/natureimmunology/
Reprints and permissions information is available online at http://npg.nature.com/reprintsandpermissions/

1. Steinman, R.M., Hawiger, D. & Nussenzweig, M.C. Tolerogenic dendritic cells. *Annu. Rev. Immunol.* **21**, 685–711 (2003).
2. Kelsall, B.L. & Leon, F. Involvement of intestinal dendritic cells in oral tolerance, immunity to pathogens, and inflammatory bowel disease. *Immunol. Rev.* **206**, 132–148 (2005).

3. Bilsborough, J., George, T.C., Norment, A. & Viney, J.L. Mucosal $CD8\alpha^+$ DC, with a plasmacytoid phenotype, induce differentiation and support function of T cells with regulatory properties. *Immunology* **108**, 481–492 (2003).
4. Asselin-Paturel, C., Brizard, G., Pin, J.J., Briere, F. & Trinchieri, G. Mouse strain differences in plasmacytoid dendritic cell frequency and function revealed by a novel monoclonal antibody. *J. Immunol.* **171**, 6466–6477 (2003).
5. Iwasaki, A. & Kelsall, B.L. Freshly isolated Peyer's patch, but not spleen, dendritic cells produce interleukin 10 and induce the differentiation of T helper type 2 cells. *J. Exp. Med.* **190**, 229–239 (1999).
6. Macpherson, A.J. & Uhr, T. Induction of protective IgA by intestinal dendritic cells carrying commensal bacteria. *Science* **303**, 1662–1665 (2004).
7. Mora, J.R. *et al.* Generation of gut-homing IgA-secreting B cells by intestinal dendritic cells. *Science* **314**, 1157–1160 (2006).
8. Coombes, J.L. & Maloy, K.J. Control of intestinal homeostasis by regulatory T cells and dendritic cells. *Semin. Immunol.* **19**, 116–126 (2007).
9. Annacker, O. *et al.* Essential role for CD103 in the T cell-mediated regulation of experimental colitis. *J. Exp. Med.* **202**, 1051–1061 (2005).
10. Sun, C.M. *et al.* Small intestine lamina propria dendritic cells promote de novo generation of Foxp3 T reg cells via retinoic acid. *J. Exp. Med.* **204**, 1775–1785 (2007).
11. MacPherson, G.G., Jenkins, C.D., Stein, M.J. & Edwards, C. Endotoxin-mediated dendritic cell release from the intestine. Characterization of released dendritic cells and TNF dependence. *J. Immunol.* **154**, 1317–1322 (1995).
12. Jang, M.H. *et al.* CCR7 is critically important for migration of dendritic cells in intestinal lamina propria to mesenteric lymph nodes. *J. Immunol.* **176**, 803–810 (2006).
13. Johansson-Lindbom, B. *et al.* Functional specialization of gut $CD103^+$ dendritic cells in the regulation of tissue-selective T cell homing. *J. Exp. Med.* **202**, 1063–1073 (2005).
14. Coombes, J.L. *et al.* A functionally specialized population of mucosal $CD103^+$ DCs induces $Foxp3^+$ regulatory T cells via a TGF-β and retinoic acid-dependent mechanism. *J. Exp. Med.* **204**, 1757–1764 (2007).
15. Denning, T.L., Wang, Y.C., Patel, S.R., Williams, I.R. & Pulendran, B. Lamina propria macrophages and dendritic cells differentially induce regulatory and interleukin 17–producing T cell responses. *Nat. Immunol.* **8**, 1086–1094 (2007).
16. Akira, S., Uematsu, S. & Takeuchi, O. Pathogen recognition and innate immunity. *Cell* **124**, 783–801 (2006).
17. Abreu, M.T., Fukata, M. & Arditi, M. TLR signaling in the gut in health and disease. *J. Immunol.* **174**, 4453–4460 (2005).
18. Uematsu, S. *et al.* Detection of pathogenic intestinal bacteria by Toll-like receptor 5 on intestinal $CD11c^+$ lamina propria cells. *Nat. Immunol.* **7**, 868–874 (2006).
19. Pavli, P., Woodhams, C.E., Doe, W.F. & Hume, D.A. Isolation and characterization of antigen-presenting dendritic cells from the mouse intestinal lamina propria. *Immunology* **70**, 40–47 (1990).
20. van Egmond, M. *et al.* IgA and the IgA Fc receptor. *Trends Immunol.* **22**, 205–211 (2001).
21. Suzuki, K., Ha, S.A., Tsuji, M. & Fagarasan, S. Intestinal IgA synthesis: a primitive form of adaptive immunity that regulates microbial communities in the gut. *Semin. Immunol.* **19**, 127–135 (2007).
22. Tseng, J. Transfer of lymphocytes of Peyer's patches between immunoglobulin allotype congenic mice: repopulation of the IgA plasma cells in the gut lamina propria. *J. Immunol.* **127**, 2039–2043 (1981).
23. Tseng, J. A population of resting IgM-IgD double-bearing lymphocytes in Peyer's patches: the major precursor cells for IgA plasma cells in the gut lamina propria. *J. Immunol.* **132**, 2730–2735 (1984).
24. Fagarasan, S., Kinoshita, K., Muramatsu, M., Ikuta, K. & Honjo, T. *In situ* class switching and differentiation to IgA-producing cells in the gut lamina propria. *Nature* **413**, 639–643 (2001).
25. Suzuki, K., Meek, B., Doi, Y., Honjo, T. & Fagarasan, S. Two distinctive pathways for recruitment of naive and primed IgM^+ B cells to the gut lamina propria. *Proc. Natl. Acad. Sci. USA* **102**, 2482–2486 (2005).
26. Kunisawa, J. *et al.* Sphingosine 1-phosphate regulates peritoneal B-cell trafficking for subsequent intestinal IgA production. *Blood* **109**, 3749–3756 (2007).
27. Macpherson, A.J. *et al.* A primitive T cell-independent mechanism of intestinal mucosal IgA responses to commensal bacteria. *Science* **288**, 2222–2226 (2000).
28. Litinskiy, M.B. *et al.* DCs induce CD40-independent immunoglobulin class switching through BLyS and APRIL. *Nat. Immunol.* **3**, 822–829 (2002).
29. Tezuka, H. *et al.* Regulation of IgA production by naturally occurring TNF/iNOS-producing dendritic cells. *Nature* **448**, 929–933 (2007).
30. Muramatsu, M. *et al.* Class switch recombination and hypermutation require activation-induced cytidine deaminase (AID), a potential RNA editing enzyme. *Cell* **102**, 553–563 (2000).
31. Kang, H.S. *et al.* Signaling via LTβR on the lamina propria stromal cells of the gut is required for IgA production. *Nat. Immunol.* **3**, 576–582 (2002).
32. Hieshima, K. *et al.* CC chemokine ligands 25 and 28 play essential roles in intestinal extravasation of IgA antibody-secreting cells. *J. Immunol.* **173**, 3668–3675 (2004).
33. Ivanov, I.I. *et al.* The orphan nuclear receptor $RORγt$ directs the differentiation program of proinflammatory IL-17$^+$ T helper cells. *Cell* **126**, 1121–1133 (2006).
34. Korn, T. *et al.* IL-21 initiates an alternative pathway to induce proinflammatory T_H17 cells. *Nature* **448**, 484–487 (2007).
35. Nurieva, R. *et al.* Essential autocrine regulation by IL-21 in the generation of inflammatory T cells. *Nature* **448**, 480–483 (2007).
36. Zhou, L. *et al.* IL-6 programs T_H-17 cell differentiation by promoting sequential engagement of the IL-21 and IL-23 pathways. *Nat. Immunol.* **8**, 967–974 (2007).
37. Bettelli, E. *et al.* Reciprocal developmental pathways for the generation of pathogenic effector T_H17 and regulatory T cells. *Nature* **441**, 235–238 (2006).
38. Mucida, D. *et al.* Reciprocal TH17 and regulatory T cell differentiation mediated by retinoic acid. *Science* **317**, 256–260 (2007).
39. Elias, K.M. *et al.* Retinoic acid inhibits Th17 polarization and enhances FoxP3 expression through a Stat-3/Stat-5 independent signaling pathway. *Blood* **111**, 1013–1020 (2008).
40. Schambach, F., Schupp, M., Lazar, M.A. & Reiner, S.L. Activation of retinoic acid receptor-α favours regulatory T cell induction at the expense of IL-17-secreting T helper cell differentiation. *Eur. J. Immunol.* **37**, 2396–2399 (2007).
41. Iwata, M. *et al.* Retinoic acid imprints gut-homing specificity on T cells. *Immunity* **21**, 527–538 (2004).
42. Viney, J.L., Mowat, A.M., O'Malley, J.M., Williamson, E. & Fanger, N.A. Expanding dendritic cells in vivo enhances the induction of oral tolerance. *J. Immunol.* **160**, 5815–5825 (1998).
43. Williamson, E., Westrich, G.M. & Viney, J.L. Modulating dendritic cells to optimize mucosal immunization protocols. *J. Immunol.* **163**, 3668–3675 (1999).
44. Macpherson, A.J. & Harris, N.L. Interactions between commensal intestinal bacteria and the immune system. *Nat. Rev. Immunol.* **4**, 478–485 (2004).
45. Niess, J.H. *et al.* CX3CR1-mediated dendritic cell access to the intestinal lumen and bacterial clearance. *Science* **307**, 254–258 (2005).
46. Chieppa, M., Rescigno, M., Huang, A.Y. & Germain, R.N. Dynamic imaging of dendritic cell extension into the small bowel lumen in response to epithelial cell TLR engagement. *J. Exp. Med.* **203**, 2841–2852 (2006).
47. Kolls, J.K. & Linden, A. Interleukin-17 family members and inflammation. *Immunity* **21**, 467–476 (2004).
48. Yokota, Y. *et al.* Development of peripheral lymphoid organs and natural killer cells depends on the helix-loop-helix inhibitor Id2. *Nature* **397**, 702–706 (1999).
49. Kopf, M. *et al.* Impaired immune and acute-phase responses in interleukin-6-deficient mice. *Nature* **368**, 339–342 (1994).
50. Barnden, M.J., Allison, J., Heath, W.R. & Carbone, F.R. Defective TCR expression in transgenic mice constructed using cDNA-based α- and β-chain genes under the control of heterologous regulatory elements. *Immunol. Cell Biol.* **76**, 34–40 (1998).

Journal of General Virology (2008), **89**, 3144–3149 DOI 10.1099/vir.0.2008/004820-0

Short Communication

Substitution of the myristoylation signal of human immunodeficiency virus type 1 $Pr55^{Gag}$ with the phospholipase C-δ1 pleckstrin homology domain results in infectious pseudovirion production

Emiko Urano,[1,2] Toru Aoki,[1] Yuko Futahashi,[1] Tsutomu Murakami,[1] Yuko Morikawa,[2] Naoki Yamamoto[1] and Jun Komano[1]

Correspondence
Jun Komano
ajkomano@nih.go.jp

[1]AIDS Research Center, National Institute of Infectious Diseases, 1-23-1 Toyama, Shinjuku-ku, Tokyo 162-8640, Japan

[2]Kitasato Institute of Life Sciences, Kitasato University, Shirokane 5-9-1, Minato-ku, Tokyo 108-8641, Japan

The matrix domain (MA) of human immunodeficiency virus type 1 $Pr55^{Gag}$ is covalently modified with a myristoyl group that mediates efficient viral production. However, the role of myristoylation, particularly in the viral entry process, remains uninvestigated. This study replaced the myristoylation signal of MA with a well-studied phosphatidylinositol 4,5-biphosphate-binding plasma membrane (PM) targeting motif, the phospholipase C-δ1 pleckstrin homology (PH) domain. PH–Gag–Pol PM targeting and viral production efficiencies were improved compared with Gag–Pol, consistent with the estimated increases in Gag–PM affinity. Both virions were recovered in similar sucrose density-gradient fractions and had similar mature virion morphologies. Importantly, PH–Gag–Pol and Gag–Pol pseudovirions had almost identical infectivity, suggesting a dispensable role for myristoylation in the virus life cycle. PH–Gag–Pol might be useful in separating the myristoylation-dependent processes from the myristoylation-independent processes. This the first report demonstrating infectious pseudovirion production without myristoylated $Pr55^{Gag}$.

Received 11 June 2008
Accepted 20 August 2008

The N-terminal region [$p17^{MA}$, matrix (MA) domain] of human immunodeficiency virus type 1 (HIV-1) $Pr55^{Gag}$ (Gag), a structural protein with multiple roles in the virus life cycle (Swanstrom & Wills, 1997), is covalently modified with a myristyol group that aids in plasma membrane (PM) targeting. Removal of this region leads to inefficient Gag targeting to the PM, resulting in dramatically reduced virus production (Bryant & Ratner, 1990; Göttlinger *et al.*, 1989; Pal *et al.*, 1990; Zhou *et al.*, 1994). Although viral particles can be produced by substituting MA with heterologous PM-targeting motifs, such substitution mutants show markedly reduced infectivity (Jouvenet *et al.*, 2006; Scholz *et al.*, 2008), probably due to an active role of MA in viral entry (Kiernan *et al.*, 1998; Wang *et al.*, 1993). However, direct experimental evidence of a viral entry-specific role for MA myristoylation is lacking. Such specific roles of Gag myristoylation can only be determined by separating the myristoylation-dependent PM-targeting function from other MA-associated functions.

We constructed a mutant *gag* expression plasmid where the myristoylated region of Gag was replaced with the N-terminal pleckstrin homology (PH) domain of phospholipase C-δ1 (PLCδ1), a well-studied cellular PM-targeting motif that functions similarly to the myristoyl moiety. PLCδ1 is a member of a family of inositol phospholipid-specific PLC isozymes involved in transducer-mediated intracellular responses (Berridge, 1993). The ~120 aa PH domain can bind to phosphatidylinositol 4,5-biphosphate [PI(4,5)P(2)] and localize to the PM with high affinity and specificity (Ferguson *et al.*, 1995b; Fiorentini *et al.*, 2006; Harlan *et al.*, 1994, 1995; Rhee, 2001; Yagisawa *et al.*, 1994), and green fluorescent protein-bound PLCδ1 PH domains have been used to visualize the PM in living cells (Stauffer *et al.*, 1998; Tall *et al.*, 2000).

We used a codon-optimized HIV-1 *gag–pol* expression vector (p*gag–pol*) for genetic modification of *gag*, as p*gag–pol* increases Gag expression and facilitates protein analyses (Wagner *et al.*, 2000). The substituted mutant retained an intact MA, with the exception of two N-terminal amino acid mutations (ATG→CTG and GGC→GCG), resulting in an MG→LA mutation to knock out the myristoylation signal of Gag and prevent internal translational initiation (Fig. 1a). The PLCδ1 PH domain residues 1–175 (Stauffer *et al.*, 1998) were linked to the LA–Gag N terminus by the amino acids PRAEFT, creating a PH–*gag–pol* expression vector (pPH-*gag-pol*, Fig. 1a). A control PH domain

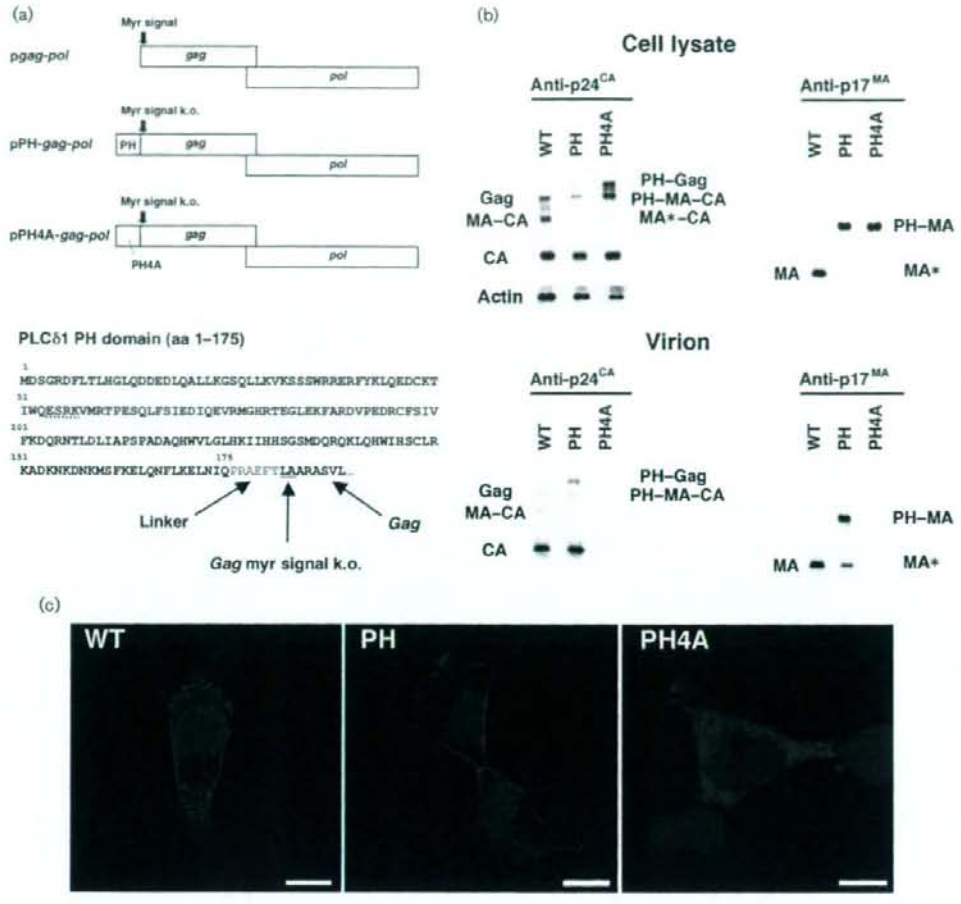

Fig. 1. Viral production by the *gag–pol* expression vectors. (a) The genetic structure of the p*gag-pol*, pPH-*gag-pol* and pPH4A-*gag-pol* expression vectors, and the amino acid sequence of the PH–Gag junction are shown. The N-terminal PH domain of PLCδ1 (aa 1–175) was fused to LA–Gag, linked by a 5 aa spacer (shown in grey). The MG→LA mutation to knock out the myristoylation signal of Gag (myr signal k.o.) is underlined. Four alanine mutations were introduced to replace the ESRK sequence (dotted line) to create the PH4A mutant. (b) Protein expression from p*gag-pol* (WT), pPH-*gag-pol* (PH) and pPH4A-*gag-pol* (PH4A) in transfected 293T cell lysates and Gag cleavage in the virions were examined by Western blot analysis using anti-$p24^{CA}$ or anti-$p17^{MA}$ antibodies. Note that the anti-$p17^{MA}$ antibody recognizes the cleaved $p17^{MA}$ protein only. The band denoted as PH–MA–CA in the virion detected by the anti-$p24^{CA}$ antibody (lower left panel) possibly overlaps with a faint Gag signal derived from PH–Gag and PH4A–Gag from which the PH and PH4A domains have been cleaved. (c) Immunofluorescence assay showing the distribution of Gag, PH–Gag and PH4A–Gag in 293T cells transfected with the respective expression plasmid. Red and blue represent $p24^{CA}$ and the Hoechst 33258-stained nucleus, respectively. Bars, 10 μm.

mutant (PH4A) had mutations at aa 54–57 (ESRK→AAAA; Fig. 1a); these residues are responsible for the PH domain–PI(4,5)P(2) interaction (Ferguson *et al.*, 1995a). PH–Gag, PH4A–Gag and their cleaved products were detected in transfected 293T cell lysates with mouse monoclonal antibodies specific for the $p24^{CA}$ (capsid) domain (anti-$p24^{CA}$; NIH AIDS Research and Reference Reagent Program) and MA domain (anti-$p17^{MA}$; Advanced Biotechnologies) (Fig. 1b). PH–Gag cleavage was more efficient than that of Gag, suggesting efficient PM targeting of PH–Gag (Fig. 1b). The Gag protein levels in the pPH4A-*gag-pol*-transfected cell lysate were higher than those in p*gag-pol*- and pPH-*gag-pol*-transfected cell lysates when adjusted for the amount of protein loaded, indicating the low virus-like particle (VLP) production efficiency by PH4A–Gag (Fig. 1b).

The intracellular distribution of Gag, PH–Gag and PH4A–Gag was analysed by immunofluorescence microscopy of transfected 293T cells (Fig. 1c). Transfected cells were grown for 24 h, fixed (4 % formaldehyde), permeabilized (0.1 % Triton X-100 for 5–30 min) and incubated with mouse anti-$p24^{CA}$ and goat anti-mouse antibodies (GE Healthcare Bio-Sciences) conjugated to streptavidin–Alexa Fluor 555 (Invitrogen). Cells were stained with Hoechst 33258, mounted and analysed using confocal microscopy as described previously (Futahashi *et al.*, 2007). Gag was found to be distributed throughout the cytoplasm and at the cell periphery. In contrast, PH–Gag signals were mostly detected at the cell periphery and PH4A–Gag was distributed homogeneously in the cytoplasm. These data clearly showed that PH–Gag targeted the PM more efficiently than Gag, consistent with the Western blot analysis (Fig. 1b). These results also suggested that the efficient PM targeting of PH–Gag depends on the ability of the PH domain to bind PI(4,5)P(2). Similar observations were made in NP2 and COS7 cells.

VLP production was also examined. Tissue culture supernatants of p*gag-pol*-, pPH-*gag-pol*- or pPH4A-*gag-pol*-transfected 293T cells were passed through nitrocellulose filters (0.45 μm) and the virions were collected by centrifugation (541 000 ***g*** for 1 h). Viral antigens, except for PH4A, were detected with anti-$p24^{CA}$ and anti-$p17^{MA}$ antibodies (Fig. 1b). Gag and PH–Gag were further processed by the viral proteases in the virions compared with the cell lysates, as indicated by the increased signals for CA and MA relative to Gag. Interestingly, approximately one-fifth of the PH–Gag in the virion was cleaved close to the PH–MA junction. Presumably, the amino acid sequence at the C end of the PH domain ELQN/FLKE (aa 164–171, where the protease cleaves at the N–F junction) served as a viral protease recognition site as it matched the substrate consensus sequence and resembled the NC–*p1* junction, RQAN/FLGK (de Oliveira *et al.*, 2003; Swanstrom & Wills, 1997). Alternatively, the N terminus of LA–Gag (EFTL/AADS) might be targeted by the viral protease. Thus, the MA released from PH–MA, designated MA*, possibly has 10 aa attached to its N terminus.

The VLP production efficiency was quantified as the concentration of CA in transfected 293T cell culture supernatants relative to that in cell lysates using a p24 ELISA (Zeptometrics). When the CA concentrations of the virion fractions were normalized to those of the cell lysates, the pPH-*gag-pol* viral production efficiency was 3.2-fold higher than that of p*gag-pol* (3.2 ± 2.0-fold, $n=14$, $P<0.001$ by Wilcoxon's matched pairs rank test; representative experiments are shown in Table 1). In contrast, pPH4A-*gag-pol* produced viral particles less efficiently than p*gag-pol* (0.09 ± 0.07-fold, $n=6$, $P<0.05$ by Wilcoxon's matched pairs rank test; representative experiments are shown in Table 1). These data were consistent with the Western blot analysis (Fig. 1b).

To characterize the physical properties of PH–Gag–Pol VLPs, we measured the specific density of virions and examined the virion morphology. Firstly, the VLPs were subjected to 20–70 % (w/w) equilibrium sucrose gradient centrifugation (120 000 ***g*** for 16 h) and fractions were recovered from the bottom to the top. The peak fraction containing the viral CA antigen was determined by p24 ELISA. Gag–Pol and PH–Gag–Pol VLPs were detected in fractions with densities of 1.15 ± 0.01 ($n=5$) and 1.16 ± 0.01 ($n=4$) g ml^{-1}, respectively (not statistically significant; representative experiments are shown in Fig. 2a). Secondly, ultrathin sections of fixed 293T cells (2 % glutaraldehyde, 2 % osmium tetroxide) transfected with p*gag-pol* or pPH-*gag-pol* were imaged by transmission electron microscopy (JEM1200EX at 80 kV or JEM2000EX at 100 kV; JEOL). The PH–Gag–Pol and Gag–Pol VLP

Table 1. Efficiency of virus production from 293T cells transfected with p*gag-pol*, pPH-*gag-pol* or pPH4A-*gag-pol* expression vector

Experiment	Plasmid	$p24^{CA}$ (ng per well)*		Virus production efficiency (B/A)	Fold increase relative to p*gag-pol*
		Cell lysate (A)	Culture supernatant (B)		
1	p*gag-pol*	4043	4869	1.204	–
	pPH-*gag-pol*	1989	8363	4.206	3.49
	pPH4A-*gag-pol*	3175	103	0.033	0.03
2	p*gag-pol*	3521	3887	1.104	–
	pPH-*gag-pol*	2638	7688	2.914	2.64
	pPH4A-*gag-pol*	5913	1125	0.190	0.17
3	p*gag-pol*	3359	4160	1.239	–
	pPH-*gag-pol*	1454	5172	3.558	2.87
	pPH4A-*gag-pol*	4226	75	0.018	0.01
4	p*gag-pol*	9666	8996	0.931	–
	pPH-*gag-pol*	4699	18273	3.889	4.18
	pPH4A-*gag-pol*	5527	534	0.097	0.10

*Cells grown in six-well plates were transfected using Lipofectamine 2000 according to the manufacturer's protocol (Invitrogen).